BOX-BEHNKEN DESIGN APPROACH TO DEVELOP NANO-VESICULAR HERBAL GEL FOR THE MANAGEMENT OF SKIN CANCER IN EXPERIMENTAL ANIMAL MODEL

TRINAYAN DEKA[*] iD, **MALAY K. DAS**[1] iD, **SANJOY DAS**[1] iD, **PUNAMJYOTI DAS**[1] iD, **L. RONIBALA SINGHA**[1] iD

¹Department of Pharmaceutical Sciences, Dibrugarh University, Dibrugarh, Assam 786004, India
*Email: trinayandeka@dibru.ac.in

ABSTRACT

Objective: To manage the increasing burden of skin cancer cases globally and to replace conventional invasive treatments and their side effects, the present study is aimed to develop a transfersomal herbal gel of Green Tea Catechins (GTC) extracted from indigenous green tea and evaluate it for *in vivo* management of skin cancer in an experimental animal model.

Methods: GTC-loaded transfersomes (GTCTF) were prepared by the thin-film hydration method. After optimizing the GTCTFs using the Box-Behnken design, they were characterized for zeta potential, structure, *in vitro* drug release, and *in vitro* skin permeation. Carbopol 940 gel was developed for the topical delivery of GTCTF and characterized for pH, viscosity, spreadability and *in vitro* skin permeation. *In vitro* MTT assay and *in vivo* chemopreventive and anticancer efficacy of the GTCTF gel were evaluated in mice.

Results: The GTCTF has shown a particle size of 151.4±1.9 nm, entrapment efficiency of 68.25±0.06 %, and drug loading of 10.41±0.02 %. The *in vitro* MTT assay in B16F10 melanoma cell lines showed promising anticancer efficacy of the GTCTF. GTCTF gel was found suitable for topical delivery with favorable pH, viscosity, spreadability, and permeability and effective in preventing and curing skin cancer in mice, with a significant reduction of tissue biochemical parameters like TNF-α, IL-1β, and IL-6.

Conclusion: Collectively, successful prevention and curing of the induced skin cancer in the experimental animal model by the GTCTF gel have established a novel herbal nanomedicine approach for the management of skin cancer.

Keywords: Skin cancer, Green tea catechins, Phytomedicine, Transfersome, Box-Behnken design, Herbal nanogel

INTRODUCTION

Skin cancer is the 13th most occurring type, with more than three lacs of new cases of deaths in 2020. Skin cancers are broadly divided into melanoma (arising from melanocyte dysfunction) and nonmelanoma skin cancers (from the epidermal derived cells) which include basal cell carcinoma and cutaneous squamous cell carcinoma [1-3]. In India, the prevalence proportion of Skin cancer is not too high like other countries [4-6]; it was around 0.70 per 100000 populations, with a 5y prevalence (all ages) up to 2020; but it is a matter of concern as the cases are increasing yearly. The north and northeast region of India has been reported to have high age-adjusted rates (AAR) of incidence of skin cancer [7, 8]. Such a burden of prevailing cases of skin cancer entices researchers to find out novel strategies for their management. Major problems with conventional therapy are the invasiveness of surgery, radiation therapy and the failure to achieve proper penetration into the deeper layers of proliferative skin ad systemic toxicity by topical chemotherapy and immunomodulatory agent [9-11]. This situation compels the researchers to develop alternative strategies for local drug delivery with minimum or fewer side effects. Natural products based on phytochemicals have displayed promising as anticancer lead molecules for skin cancers [12-14]. Among the phytochemicals, Green tea catechins (GTC) are a group of polyphenolic (flavan-3-ols) compounds available in *Camellia sinensis* that were known for their cancer chemopreventive and chemotherapeutic effects. The four major green tea catechins (GTCs) are (−)-epicatechin (EC), (−)-epigallocatechin (EGC), (−)-epicatechin-3-gallate (ECG), and (−)-epigallocatechin-3-gallate (EGCG), among which EGCG has received considerable attention for its inhibitory activities against carcinogenesis at all stages, viz. initiation, promotion and progression [15]. GTC have shown preventive action against both UVA and UVB-radiation-induced skin cancers in mice [16]. In an *in vitro* anti-cancer study, around 400 µg/ml of GTC aqueous extract was found successful to achieve half-minimal inhibitory concentration [17]. While a 6 mg topical dose of green tea extract have showed promising protection against induction of skin

papillomas in mice [18]. Studies on *in vitro* and *in vivo* experiments have sustained the functions of catechin for suppressing tumorigenesis in a number of carcinogenic animal models, as well as in several human cancer cell lines like SKOV-3, HCT-15, Hs-578T, H-1299, CL-13 cells [19-22]. However, the efficacy of catechins *in vivo* and *in vitro* is inconsistent; such dispersity may be attributed to the low bioavailability, low permeability, instability and the weak targeting ability of catechin in cancers [22, 23].

Nanotechnology-based delivery systems have emerged as powerful aids that can enhance stability. Solubility the bioavailability of phytochemicals like GTCs. They can also achieve targeted delivery when modified with targeting molecules [25-27], and also can improve therapeutic efficacy by enhancing the bioavailability and stability and significantly enhance the anti-skin cancer efficacy and stability of EGCG and GTCs, by protecting the GTC's degradation in tissue's microenvironment [28-31]. Recently vesicular nanocarriers, mainly transfersomes or deformable liposomes, have gained much attention owing to their tailored membrane functionalities, including self-adaptable, ultra-flexible, more elastic in nature and high radius of curvature etc., which were found suitable for effective skin delivery [32, 33]. Due to the hydrophilic nature, they tend to avoid skin dehydration and in order to remain swollen or hydrated, they penetrate over the skin pores to the deeper, more hydrated skin layers. Also, transfersomes can persuasively conserve the drug from undesirable absorption into cutaneous blood vessels and are moderate to confining the active therapeutic agents throughout the skin cells [34, 35].

Therefore, the present investigation was aimed to develop and characterize the green tea catechin-loaded transfersomal gel formulations (GTCTF), using the Box-Behnken design for optimization for the successful management of skin cancer both *in vitro* and *in vivo*.

MATERIALS AND METHODS

Materials

Raw green tea leaves were procured from Zaroni Green Tea. Ltd., Assam, India. Soya phosphatidylcholine and sodium cholate were

procured from Himedia Pvt. Ltd., Mumbai, India. Polyphenon 60 was procured from Sigma Aldrich Pvt. Ltd., Saint Louis, USA. (-)-Epicatechin and (-)-Epigallocatechin gallate (EGCG) were procured from Cayman Chemical Company, Michigan, USA. (-)-Catechin gallate was procured from Santa Cruz Biotechnology, Inc., Texas, USA. ELISA (mouse tissue lysate) kits for TNFα, IL-6 and IL-1β were procured from RayBiotech Life, Inc., Georgia, USA. All other reagents and chemicals used were of analytical grade. Instead of using any of the single catechin compounds, GTC extract is being used as a drug because mixtures of catechins was observed to have better anti-tumor activity than pure EGCG or any other catechin owing to their synergistic effect [36].

Extraction and standardization of green tea catechins

10 g of green tea leaves were extracted with 300 ml of pure water at 80 °C for 40 min. The infusion was then filtered using 11 μm pore-sized filter paper (Whatman® qualitative filter paper, Grade 1). The aqueous tea infusion was initially partitioned with chloroform (three-time) for the maximum removal of caffeine and then with an equal volume of ethyl acetate (three-time). Finally, the aqueous extract was evaporated using a rotary evaporator (RV10, IKA, Germany), down to 20 ml, lyophilized (temperature-80 °C and pressure 0.02 mbar) using a lyophilizer (SS1-LYO, Southern Scientific Lab Instruments, India) and the resulting solid was weighed. The extracted green tea catechin (GTC) was standardized using UV-Vis spectroscopy, FT-IR spectroscopy and HPTLC methods. Absence of caffeine was confirmed by Murexide test [37-39]. UV-Vis spectroscopy (UV 1800, Shimadzu, Japan) was used to obtain the λmax of GTC and polyphenon 60 for comparison. FT-IR spectroscopy (Alpha, Bruker, Germany) was used to get the FT-IR spectrum of GTC and polyphenon 60 for the confirmation of the presence of characteristic peaks in the extracted GTC sample. For HPTLC (CAMAG, Switzerland), samples were prepared in methanol: water (4:1) as the solvent, a mixture of toluene, acetone, formic acid (9:9:1) used as mobile phase and HPTLC Si 60 F_{254} plates (Merck) was used as stationary phase [40, 41].

Design of box-behnken model for the optimization of GTC-loaded transfersomes (GTCTF)

To statistically optimize of the formulation of GTC-loaded transfersomes, the Box–Behnken Design (BBD), one of the response surface methodology (RSM) tools was used [41]. This Design of Experiment (DoE) was constructed using Design-Expert software (Version 10.0.1, Stat-Ease Inc. USA). In this design, three factors at three levels (3^3) were being considered, where independent variables (factors) were the amount of soya phosphatidylcholine (SPC) (A), amount of sodium cholate (SC) (B) and amount of GTC (C), for preparation of the GTCTFs, with three levels being high (+1), medium (0) and low (-1) as demonstrated in table 1.

Table 1: Box-behnken design for GTCTF formulations showing the level of variation of the variables

Independent variables	Character	Level of variation		
		-1	0	+1
Amount of SPC (mg)	A	65	75	85
Amount of SC (mg)	B	5	15	25
Amount of GTC (mg)	C	5	10	15

After formulating the GTCTFs using these three variables, the dependent variable or the responses evaluated were Particle Size or Effective Diameter (ED) (Y_1), Polydispersity Index (PDI) (Y_2), Drug Entrapment Efficiency (EE %) (Y_3), and Drug Loading (DL %) (Y_4). A total of 17 Formulations were obtained from software to get an ultimate optimized GTCTF formulation. The optimized formulation was selected using the point prediction method in the software. The predicted responses of the optimized formulation were further confirmed by comparing with experimental response values.

Preparation of GTCTFs

GTCTFs were prepared by the thin film/lipid film hydration method [42]. The specified amount of SPC and SC (table 2 and table 4) were dissolved in 20 ml of solvent mixture chloroform and methanol at a ratio of 3:1. The solution was then subjected to evaporation under the vacuum at 50 °C, using a rotary evaporator (RV 10, IKA, Germany). After complete evaporation of the solvent, a thin film of lipid was found to be formed at the inside bottom surface of the evaporation flask. Then the specified amount of GTC solution in phosphate buffer (pH 6.8) was poured slowly into the flask and left for hydration and swelling of transfersomes with mild agitation at 50 °C to obtain the GTCTF dispersion. The GTCTF dispersion was then sonicated for 30 to 35 min using a bath sonicator (UCB 30, Spectralab Instruments, India) to get homogenized GTCTF dispersion.

Evaluation of characteristic parameters of GTCTF

Compatibility studies of GTC and other transfersomal components

To determine any incompatibility among the components of the GTCTF formulation, FT-IR and DSC studies of the individual component, the physical mixture of the components and the lyophilized formulation were done [43]. In the FT-IR study, an individual sample was placed over the sample plate of the FT-IR spectrometer (Alpha, Bruker, Germany) and the covering probe was placed over the sample. FT-IR spectrum of the samples was obtained over a wavenumber region of 400 to 4000 cm⁻¹ to record the characteristic peaks. DSC thermogram of the samples were recorded with a Differential Scanning Colorimeter (DSC 4000, Perkin Elmer, USA) which was calibrated using indium as the standard. For the DSC study, 5-10 mg of the sample was placed in the alumina crucible and heated from 30 to 445 °C, with a nitrogen flow of 50 ml/min; at a heating rate of 10 °C/min. The analysis of the DSC thermogram was done visually and compared with references from the literature [44, 45].

Particle size and zeta potential

Freshly prepared optimized GTCTF was diluted to 100 times in double-distilled water for the measurements. The average particle size/effective diameter (ED) and polydispersity index (PDI) of the formulations were measured by a particle size analyzer (90 Plus, Brookhaven Instruments, USA). The zeta potential of the formulations was measured by Zetasizer (Nano ZS, Malvern Instruments, UK). The particle size of the GTCTFs was measured at a 90° scattering angle using Dynamic Light Scattering. The zeta potential of the GTCTFs was measured by using laser Doppler micro-electrophoresis [46].

Drug entrapment efficiency (EE %) and drug loading (DL %)

The entrapment efficiency (EE %) of the GTCTFs was determined using the size exclusion chromatography method. To get the amount of entrapped drug in the GTCTF, the amount of free drug was subtracted from the total amount of drug added initially in the formulation [47]. The amount of free GTCs was determined spectrophotometrically at 273 nm using UV-Vis Spectrophotometer (UV 1800, Shimadzu, Japan). Phosphate Buffer pH 6.8 was treated as blank. The % EE was calculated by the formula below:

$$\% \text{ Entrapment Efficiency} = \frac{(\text{Amount of GTC added} - \text{Amount of free GTC})}{\text{Amount of GTC Added}} \times 100 \; \text{.......} \; (1)$$

To determine drug loading, the GTCTF dispersion, free of unentrapped GTC, was lyophilized using lyophilizer (SS1-LYO, Southern Scientific Lab Instruments, India). The weight of the dried sample was determined from the tare weight of the vessel and the final weight of the vessel. [47] The DL % was calculated by the formula below:

$$\% \text{ Drug Loading} = \frac{\text{Amount of GTC added} - \text{Amount of free GTC}}{\text{Weight of the dried GTCTF}} \times 100 \ \dots\dots (2)$$

High-resolution transmission electron microscopy (HRTEM)

The shape and size of the optimized GTCTF were studied using a high-resolution transmission electron microscope (JEM-2100, JEOL, Japan). One drop from the 100-times diluted sample with deionized water was deposited on a carbon film-covered copper grid to form a thin-film specimen. The solvent was then evaporated by air dry, keeping undisturbed overnight. Then the sample was examined under the microscope and microphotographs were taken [48].

Degree of deformability

The optimized GTCTF preparation was passed through polycarbonate filters of sizes 200 nm and 100 nm subsequently. Vesicles retained on each filter were studied for particle size and distribution by the DLS technique after keeping undisturbed for 2 h, as mentioned in the section of particle size and zeta potential. The degree of deformability (D) can be calculated by the following equation:

$$D = J \times \frac{rv}{rp} \ \dots\dots\dots (3)$$

Where J = amount of GTCTF dispersion extruded during 5 min, rv = the size of the vesicle after extrusion, rp = pore size of the filter [47].

In vitro drug release

The *in vitro* drug release study of GTCTF was performed by using Franz diffusion cell with slight modification. Cellophane membrane having a molecular weight cut-off of 12000 Da, was pre-soaked with distilled water and mounted horizontally on the receptor compartment of the Franz diffusion cell. The effective permeation area the of donor compartment exposed to the receptor compartment was 3.14 cm^2 and the capacity of the receptor compartment was 50 ml. 50 ml of phosphate buffer solution (pH 7.4) was filled into the receptor compartment, maintained at 37±0.5 °C and stirred by a magnetic bar at 100 rpm. GTCTF formulation equivalent to 2.01 mg of GTC was placed on the donor compartment and the top of the diffusion cell was covered. At appropriate time intervals (1, 2, 3, 4, 5, 6, 7, 8, 9, 10, 11, 24, 30, 48, 56 and 72 h), 1 ml aliquots of the receptor medium were withdrawn and immediately replaced by an equal volume of fresh phosphate buffer (pH 6.8) to maintain sink conditions. The samples were analyzed spectrophotometrically at 273 nm using UV-Vis Spectrophotometer (UV 1800, Shimadzu, Japan) [48].

In vitro skin permeation study of GTC and GTCTF

The *in vitro* skin permeation study was performed for free GTC and GTCTF for maximum permeation by the same procedure as described in the section of *in vitro* drug release, where instead of cellophane membrane, excised pig ear skin was used. The skin was excised from adult domestic pig ears, obtained from a local commercial supplier. After thorough washing and hair removal, the skin was carefully separated from cartilage using a scalpel. Subsequently, subcutaneous adipose tissues were removed; while maintaining a 1 mm thickness for all the samples with a Vernier. After being dried with a tissue, the skin was immediately mounted on the diffusion cells or frozen at-20 °C for a maximum period of 4 w [48, 49].

Stability studies of optimized GTCTF

The stability of the optimized GTCTF was investigated in accordance with the ICH guidelines by measuring some parameters such as vesicle size, PDI, % EE after specific storage conditions. Samples from the optimized GTCTF formulation were stored in tightly closed containers and kept at two different conditions: 4±1 °C and at 25±1 °C with 60±5 % RH for 6 mo [48].

Preparation of GTCTF gel

The GTC-loaded Transfersomal gel of 3 % w/w drug concentration was prepared by using Carbopol 940 (1.5 % w/w) as a gelling agent. Other components used in the preparation were glycerin 5 % w/w, methylparaben 0.1 % w/w, triethanolamine (TEA) and double-distilled water q. s. Required amount of Carbopol 940 was dispersed in 10 ml double distilled water. After complete dispersion, 1.5 % Carbopol 940 solution was kept for 24 h at room temperature for swelling. A specified amount of glycerin and methylparaben was mixed with the gel. Triethanolamine was added to it dropwise [49]. An appropriate amount of optimized GTCTF (3 % w/w) was then incorporated into the gel base with gentle stirring.

Characterization of GTCTF gel

Physical inspection

The developed GTCTF was inspected visually to assess the homogeneity of the formulations [49].

Estimation of pH value

The pH measurement of GTCTF gels was investigated using a calibrated digital pH meter (pHTestr 10, Eutech Instruments, Singapore) at room temperature [49]. The pH measurement was done in triplicate and the average reading was taken.

Spreadability test

This test was evaluated to determine the spreadability of the GTCTF gel and measure the diameters of spreading when applied to the affected area. The test is done by using the horizontal plate method; by spreading 0.5 g of the GTCTF gel on a circle of 2 cm diameter pre-drawn on a glass plate and then a second glass plate was placed. 500 g of weight was permitted to rest on the upper glass plate for 5 min and then the distance spread by the gel from the drawn circumference was measured [50].

Viscosity study

The viscosity of the GTCTF gel was determined by using a digital viscometer (Brookfield Engineering Laboratories, USA). Spindle no. 64 was used to evaluate the viscosity of the prepared GTCTF gel at a rotation speed of 0.3 rpm [49].

Drug content determination

Accurately, an amount of GTCTF gel preparations equivalent to 1 mg of GTC was diluted to 10 ml using phosphate buffer pH 6.8. Then the drug content was determined spectrophotometrically at 273 nm using a UV-Vis spectrophotometer (UV 1800, Shimadzu, Japan) using a blank sample containing the same components (without drug) [49, 50]. The percentage of drug content was calculated as follows:

$$\% \text{ Drug content} = \frac{\text{Actual amount of GTC in the formulation}}{\text{Theoritical amount of GTC in the formulation}} \times 100 \ \dots (4)$$

In vitro skin permeation study of GTCTF gel

The *in vitro* skin permeation characteristics of the prepared GTCTF gel were determined using pig ear skin in the same way as mentioned in the section of *in vitro* skin permeation study of GTC and GTCTF. At the specific interval of time (1, 2, 3, 4, 5, 6, 7, 8, 9, 10, 11, 12 and 24 h), 1 ml samples were withdrawn and substituted with the fresh buffer. Samples were analyzed for the content of GTC spectroscopically at 273 nm [48, 50]. The sample from the skin permeation study was scanned between 200 nm to 400 nm using a UV-Vis spectrophotometer (UV 1800, Shimadzu, Japan). The λ_{max} of the drug appeared at 273 nm, indicating no interference by skin extract in the analysis of the drug in the permeation sample.

In vitro anticancer activity on B6F10 melanoma cells

The *in vitro* anticancer of the GTCTF was been carried out by MTT assay on B6F10 melanoma cell lines at Biocyte Institue of Research and Development, Maharashtra, India [51]. Fluorouracil (5-FU) was used as a reference standard anticancer drug. Free GTC and GTCTF were studied for MTT assay. B6F10 Cells were incubated at a concentration of 1×10^4 cells/ml in a culture medium for 24 h at 37 °C and 5 % CO$_2$. Cells were seeded at a concentration (70μl) 10^4 cells/well in 100 μl culture medium and 100 μl compounds (20 μg/ml, 40 μg/ml, 60 μg/ml, 80 μg/ml, 100 μg/ml) into micro plates respectively (tissue culture grade and 96 wells). Control wells were incubated with DMSO (0.2 % in PBS) and cell line. All samples were incubated in triplicate. Controls were maintained to determine the control cell survival and the live cells percentage after culture. Cell cultures were incubated for 24 h at 37 °C and 5 % CO$_2$ in CO$_2$

incubator. After incubation, the medium was completely removed and Added 20 µl of MTT reagent (5 mg/min PBS). After the addition of MTT, cells were incubated for 4 h at 37 °C in CO_2 incubator. Observed the wells for formazan crystal formation under the microscope. The yellowish MTT was reduced to dark-colored formazan by viable cells only. After removing the medium completely. Added 20 µl of DMSO (kept for 10 min) and incubate at 37 °C (wrapped with aluminium foil). Triplicate samples were analyzed by measuring the absorbance of each sample using a microplate reader at a wavelength of 570 nm. % Cell viabilities were calculated based on the ratio of the absorbance of the sample treatment relative to the absorbance of the control treatment. IC_{50} (half maximal inhibitory concentration) was calculated using Graph Pad Prism 7 Software. The non-linear curve fitting of data was performed using inhibitor (concentration) vs normalized response (% cell viability) to get the IC*50* values for respective samples [52].

Animal study

The protocol for general procedures and use of animals for conducting this study has been reviewed and approved by the Institutional Animal Ethics Committee, Department of Pharmaceutical Sciences, Dibrugarh University, under Approval No. IAEC/DU/156, dated.01/11/2018). The laboratory animals were obtained from the animal house facility of Regional Medical Research Centre, Dibrugarh, Assam, India. All the experiments were conducted in the animal house facility at the Department of Pharmaceutical Sciences, Dibrugarh University, Assam, India. The biochemical parameter investigation using the ELISA kit was performed at Multi-Disciplinary Research Unit at Assam Medical College and Hospital, Dibrugarh, Assam, India.

Skin irritation study

The Skin irritation study was carried out on male Albino rabbits weighing 2-2.5 kg according to the OECD guidelines 404 [53]. A total of three rabbits were used in the experiment. The animals were kept under standard laboratory conditions and housed in Steel cages, one per cage, with free access to a standard laboratory diet and water. The skin compatibility of the formulation as a topical medication cab be confirmed by this test. The dorsal hair of both sides of the rabbits was shaved. A single dose was applied to the left side of the rabbit with the right side as control. The development of erythema, which is a manifestation of cutaneous vascular dilatation, was monitored daily for 7 d. The back of each rabbit was carefully inspected for any sensitivity reaction, if any, and was recorded as: A-No reaction, B-Slight, patchy erythema (light pink), C-Moderate but patchy erythema (dark pink), D-Moderate erythema (light red) and E-Severe erythema with or without edema (extreme red) [54, 55].

***In vivo* anticancer and chemopreventive activity**

Swiss albino mice were used in anticancer and chemopreventive activity evaluation of GTCTF gel. Total of 21 mice were used as mentioned below. All the animals will be housed in the animal house under room temperature at 22 °C-25 °C under a 12 h light/12 h dark cycle in standard cages and given free access to a standard laboratory diet and water ad libitum. The dorsal skin of each animal will be shaved 2 d prior to initiation of the experiment. All the treatments will be given topically onto the shaved area on the dorsal surface of the body.

The treatment regimen and numbers of animals per group were as Group I: Normal Control, Received topical gel base only (6 animals, 3 for anticancer, 3 for chemoprevention); Group II: Cancer Control, Received inducing agent 7,12-Dimethylbenz[a]anthracene (DMBA) (3 animals for anticancer); Group III: Received topical gel after induction (3 animals for anticancer), Group IV: Received standard marketed formulation of 1% Flonida cream (Menarini India Pvt. Ltd.) after induction (3 animals for anticancer), Group V: Received inducer DMBA (3 animals for chemoprevention), Group VI: Received GTCTF gel along with inducer (3 animals for chemoprevention). For anticancer activity, animals in Group II-IV were given topical application of DMBA (25 µg in 0.1 ml of acetone) twice per week. Topical gel of green tea catechin-loaded transfersomes and 1%

Flonida cream were applied daily to the animals of Group III and IV after the induction of skin cancer, confirmed by tumor growth on the skin, respectively, until the termination of the experiment at 22 w. For the chemopreventive activity evaluation Group I was considered as a normal group that received only blank gel formulation. Group V and VI were given topical application of DMBA twice weekly, while Group VI was treated daily with GTCTF also until the 14 w. Animals of both anticancer and chemopreventive activity study were euthanized by cervical dislocation under diethyl ether anesthesia for dissection and collection of skin tissue after the termination of each experiment. A portion of the skin tissue was stored in 10 % neutral buffered formalin for histological analysis and the remaining tissue will be immediately stored at-80 °C for the analysis of other following parameters using ELISA Kit (Ray Bio® Tissue Lysate ELISA kit): Necrosis factor alpha (TNF-α) and Interleukins 1β and 6 (IL-1β, IL-6) [56-59].

Statistical analysis

The quantitative results were presented as mean±standard deviation (SD), except for optimization formulation optimization by design expert software DX 10, where values are represented as average values only. The statistical significance of the data was assessed by conducting ANOVA test or t-test using Microsoft Excel 2016 and Graph Pad Prism V7 statistical software. Statistical significance is interpreted if $p < 0.05$ [52, 57-59].

RESULTS

Extraction and standardization of GTC

The GTC extracted from green tea leaves was found to be crystalline orange-brown colored powder. Murexide test confirmed the absence of caffeine in the extract. It was hygroscopic as the materials were freeze-dried and freeze storage condition was used for further use. The percent yield of GTC was found to be 12.65 %. The extracted GTC was standardized using UV-Vis spectrum and FT-IR spectrum; Polyphenon 60 was used as the reference standard (fig. 1 and fig. 2). The presence of (-)-catechin gallate, (-)-epicatechin, and (-)-epigallocatechin gallate (EGCG) was confirmed by HPTLC chromatogram (fig. 3). The content of EGCG in the GTCs was determined by the calibration curve method using UV-Vis spectroscopy (λ_{max} 273 nm) and found to be 32.54 % w/w.

The λ_{max} of both GTC and Polyphenon 60 at around 273 nm confirms the sample identity (fig. 1). The FT-IR spectrum showed the presence of a characteristic aromatic O-H bond peak at around 3100 cm^{-1} to 3300 cm^{-1}. The other peak also confirms the identity of the GTC sample. The presence of characteristic bands in the GTCs similar to (-)-catechin gallate (CG), (-)-epicatechin (EC) and (-)-epigallocatechin gallate in the GTC sample chromatogram indicated the extraction process is successful and extracted GTC can be used as an herbal drug with such therapeutic phytochemicals.

Preparation of optimized GTCTF

The optimized GTCTF formulation was prepared by DoE using Box-Behnken experimental design. As shown in table 2 the different GTCTF formulations were prepared and analyzed for the dependent response. The analysis of the data showed the effect of independent variables on the response. The optimization was done to get high EE % and DL % in Design-Expert software. The quadratic model was found as the optimum model for all four of the dependent responses. According to the 3^3 Box-Behnken Design investigations, the amounts of lipid forming vesicles (SPC), edge activator concentration (SC) and GTC had a significant impact on the particle size/effective diameter, PDI, EE % and DL %. These observations help in the selection of independent variables in this investigation. The significance of the model was estimated by ANOVA, where, at p-value<0.05, the model was considered significant. The p-value<0.05 implies that the quadratic model is statistically significant to describe the interrelationship among the independent factors and the dependent responses. The total 17 formulations were prepared as mentioned earlier and evaluated for the responses. The complete BBD with the variables for optimizing GTCTFs are presented in table 2.
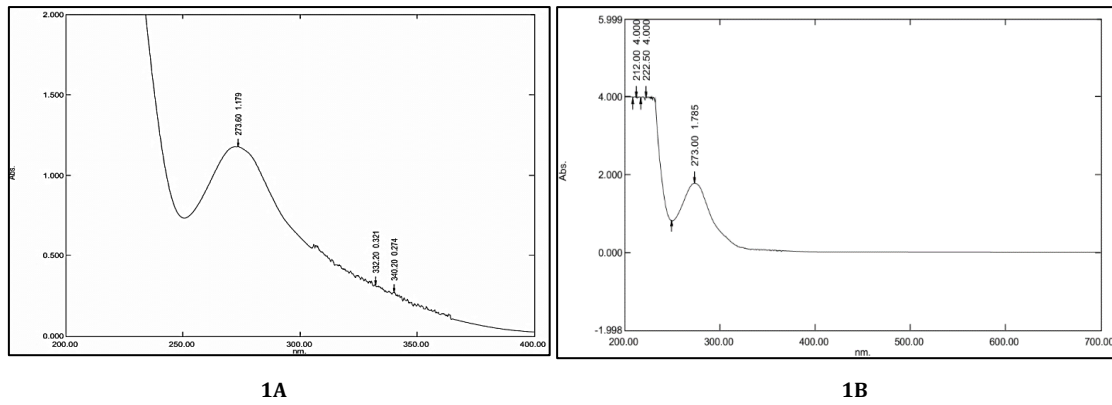
1A

1B

Fig. 1: Comparison of UV-Vis spectra. 1A: represents the UV-Vis spectrum of GTC extract and 1B: represents the UV-Vis spectrum of polyphenon 60. Both spectrum showed λ_max at around 273 nm, confirming the similarity of the two
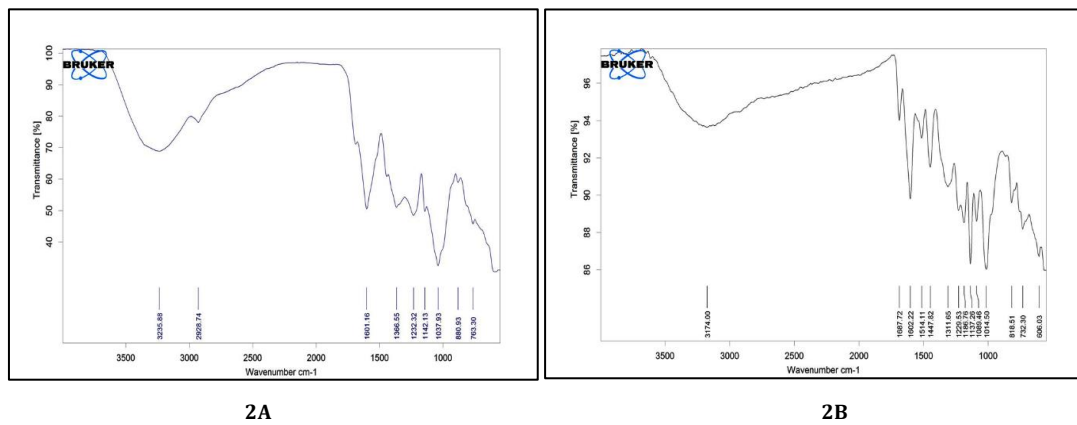

2A

2B

Fig. 2: Comparison of FT-IR spectra. 2A: represents the FT-IR spectrum of GTC extract and 2B: represents FT-IR spectrum of Polyphenon 60. It is observed that both the recorder spectrum has similar peaks at around same wave number. Presence of the same functional groups in GTC as compared to the reference Polyphenon 60 confirms the identification of the extracted material as a mixture of catechins
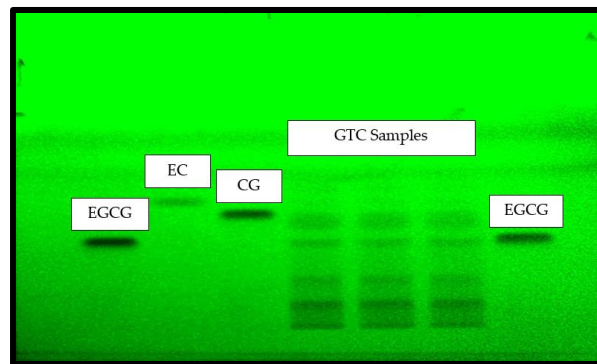

Fig. 3: Image HPTLC plate with GTC extract and standards at 254 nm, The first and the last track of the HPTLC plate was of standard EGCG, the second for epicatechin and the third for Catechin gallate. Fourth, fifth and sixth track was of extracted GTCs. The presence of bands at same height similar to the standard's band on the GTCs' tracks confirms the presence of catechins in the extracted material

Effect on particle size

In this study, it was found that the particle size or the effective diameter (ED) is influenced by the amounts of the GTCTF components. The maximum and minimum ED of the GTCTFs were found to be 395.4±5.4 nm and 137.3±1.3 nm, respectively. With the increase of SPC from 65 mg to 75 mg the ED first increases, but when it further increased to 85 mg (table 2) the size was found to be reduced (F3, F6 and F15 in table 2). Similarly, increasing the amount of SC decreases the particle size as observed for F6, F4, F16 (table 2). With the increasing amount of GTC, particle size became larger, provided with low SC and high SPC, for F12, F16, F8 (table 2). These

influences of the independent factors on particle size are represented by the contour and 3D response graphs (fig. 4).

The fitted mathematical polynomial equation in terms of actual factors derived from the BBD verified our findings as it demonstrates the synergistic effect of SPC and GTC and the antagonistic effect of SC on the dependent response ED. A positive coefficient indicates that the factor has a synergistic influence, whereas a negative value shows an antagonistic influence on the responses.

$$ED\ (Y1) = -415.34 + 13.74SPC - 12.08SC + 55.95GTC + 0.22SPC.\ SC - 0.77SPC.\ GTC - 0.96SC.\ GTC - 0.066SPC^2 - 0.05SC^2 + 0.95GTC^2 \ldots\ldots (5)$$

Table 2: The box-behnken design with independent variables that used to optimize the GTCTF and the evaluated results of responses

Run	Independent variables			Dependent variables[*]			
	SPC (mg)	SC (mg)	GTC (mg)	ED (nm)[a]	PDI%[a]	EE %[a]	DL %[a]
1	85	15	5	267.4	0.295	23.51	1.3
2	85	25	10	196.3	0.297	31.29	2.9
3	65	15	5	223.5	0.294	42.49	2.7
4	75	15	10	213.1	0.273	53.05	5.8
5	65	5	10	296.1	0.321	48.49	6.7
6	75	5	15	395.4	0.336	38.84	7.1
7	65	25	10	137.3	0.338	67.31	7.2
8	65	15	15	315.7	0.334	50.97	11.4
9	75	15	10	234.1	0.281	61.24	6.7
10	75	15	10	222.9	0.261	75.41	7.9
11	75	15	10	262.8	0.302	61.47	6.5
12	75	5	5	260.3	0.273	46.31	2.9
13	75	15	10	245.4	0.298	59.64	6.4
14	75	25	5	209.4	0.356	38.67	1.9
15	85	5	10	265.9	0.31	53.79	5.9
16	75	25	15	152.1	0.319	69.33	9.7
17	85	15	15	205.2	0.273	45.85	6.9

[*]Data are given in mean (n=3), [a]Significantly influenced by independent variables (SPC, SC and EGCG) ($p<0.05$)

Effect on PDI

It is found that the Polydispersity index of the GTCTFs was significantly affected by the formulation parameters. Increasing the amount of phospholipid results in decreasing of the PDI, whereas with an increase of the amounts of edge activator and the drug, the PDI also increases. The relationship of the formulation parameter to PDI follows a quadratic polynomial model as derived from the BBD. The highest PDI observed for formulation F14 is 0.356±0.003 and the lowest value for PDI is 0.261±0.006 for the GTCTF F10 (table 2). With the increase of SPC it was observed that the PDI decreases as in

F8, F13, F17 (table 2). On the other hand, with the PDI increases with increasing the amount of SC and GTC as observed in F12, F11, F16 in table 2). The contour and 3D response surface graphs for the parameter represent the evaluated influence of the parameters of GTCTF on PDI (fig. 5). The synergistic effect of SC and GTC, and the antagonistic effect of SPC on PDI are confirmed by the fitted quadratic equation in terms of the actual factor.

$$PDI = +0.39 - (5.8E\text{-}003)\, SPC + (3.18E\text{-}003)\, SC + 0.02\, GTC - (7.5E\text{-}005)\, SPC.SC - (3.1E\text{-}004)\, SPC.GTC - (5E\text{-}004S)\, SC.GTC + (5.75E\text{-}005)\, SPC^2 + (2.78E\text{-}004)\, SC^2 + (4.1E\text{-}004)\, GTC^2 \quad \text{............(6)}$$
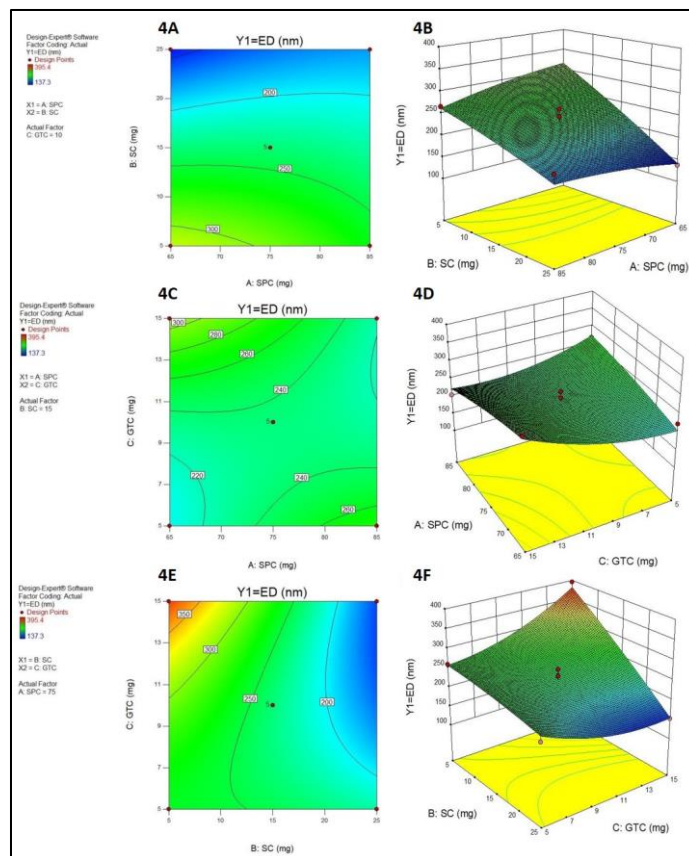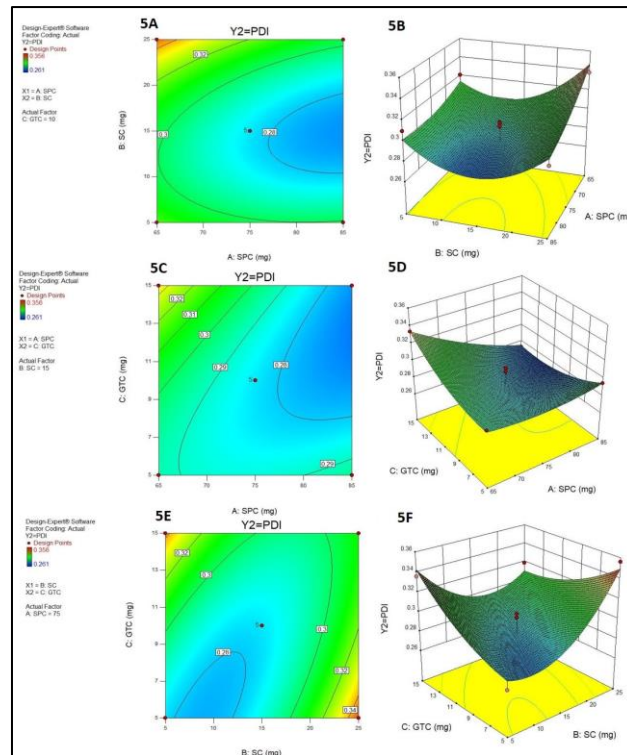

Fig. 4: Contour and response surface 3D plots showing the effects of the independent variables on particle size (Y1). Two independent variables are considered at a time, while the third one remains constant. The synergistic effect of SPC (4B, 4D) and GTC (4D, 4F), and the antagonistic effect of SC (4B, 4F) on the size of the transfersomes are displayed through the graphs

Fig. 5: Contour and response surface 3D plots showing the effects of the independent variables on PDI (Y3). Two independent variables are considered at a time, while the third one remains constant. The synergistic effect of SC (5B, 5F) and GTC (5D, 5F), and the antagonistic effect of SPC (5B, 5D) on PDI are represented by the graphs

Effect on entrapment efficiency

The entrapment efficiency is very crucial in developing nanoparticle. The amount of drug entrapped in a nanocarrier affect the drug delivery to the targeted site for the treatment of ailments. In this study, during the optimization of GTCTFs we observed that the EE % is prominently affected by the formulation components. For all the independent variables, it is observed that when their amount increases from low to medium value, the EE % increases and increasing amounts for medium to high value decreases the EE % (table 2). The maximum EE % was found 75.41 % for F10 and the minimum was observed 23.51 % for F1 as presented in table 2. The EE % increased when SPC increased from 65 mg to 75 mg (F5 and F10, table 2) and then decreased with a further increase of SPC to 85 mg (F2, table 2). Similar effect on PDI was observed when SC was increased from 5 mg to 15 mg (F12 and F10, table 2) and from 15 mg to 25 (F14, table 2). Amount of GTC also influences the EE % in the same way. While increasing the amount of GTC from 5 mg to 10 mg, EE % first increased and then further increasing GTC to 15 mg, EE % observed to be decreased (F3, F10 and F17, table 2). The correlation between the amounts of SPC, SC, GTC and the EE % of GTCTF, follows a quadratic model as suggested by the BBD. The fitting of the model is significant with p<0.05, as the variables showed a synergistic effect on EE %. The fitted quadratic equation confirms the observed influences of the independent variable of EE % (Eq. 7). The contour and 3D response surface graphs illustrates the observed findings more precisely (fig. 6).

$$EE\% = -539.99 + 14.81SPC + 6.73SC + 2.65GTC - 0.10SPC \cdot SC + 0.07SPC \cdot GTC + 0.19SC \cdot GTC - 0.09SPC^2 - 0.02SC^2 - 0.47GTC^2 \dots \dots (7)$$

Effect on drug loading

Similarly, as with the other responses, the drug loading in GTCTFs was also significantly influenced by the formulation components. The maximum 11.4 % and minimum 1.3 % loading of GTC to GTCTF was observed in F8 and F1, respectively (table 2). With an increasing amount SPC from 65 mg to 75 mg DL % increased first observed to be increased (F 5 and 6, table 2), then further increasing SPC to 85 mg, decreased the DL % (F15, table 2). Similarly, an initial increase

in SC from 5 mg to 15 mg increased the DL % (F5 and F10, table 2), which decreased with a further increase of SC to 25 mg (F2, table 2). The correlation of the amount of SPC and SC to the DL % of the GTCTFs is nonlinear; however, a direct linear relation of the amount of GTC with the DL % is observed, where increasing the amount of GTC increased the DL %, as shown in table 2. Moreover, all the variables fitted significantly to the quadratic response surface model as generated by BBD (Eq. 8). The contour plot and 3D response surface graphs of the independent variables with the response DL %, clearly demonstrate our findings on the influence of the formulation parameters on DL % (fig. 7). The polynomial equation in terms of actual factors verifies the synergistic effects of the variable on DL %.

$$DL\% = -30.17 + 0.64SPC + 0.62SC + 2.03GTC - (8.75E-003) SPC \cdot SC - 0.02SPC \cdot GTC + 0.02 SC \cdot GTC - (3.25E-003) SPC^2 - (4.99E-003) SC^2 - 0.02GTC^2 \dots \dots (8)$$

Optimization and selection of formulation parameters for GTCTF

After the analysis of the influences of each independent variable on the responses, the point prediction method in the BBD utilizing Design Expert 10 software was used to obtain the optimized parameters for the GTCTF formulation, with the criteria to obtain maximum entrapment efficiency (Y2) and drug loading (Y4). As particle size and PDI are in the acceptable range for nanoformulations, no goal was set for them in the point prediction. The optimized formulation selected from the software was composed of 65 mg of SPC (phospholipid), 25 mg of SC and 15 mg of GTC. The formulation showed particle size of 151.4±1.9 nm, PDI of 0.326±0.009, EE % of 68.25±0.06 % and DL % of 10.41±0.02 %. Confirmation of the predicted values was done by comparing the experimentally evaluated values of responses using the software. The predicted and the evaluated values of the optimized formulation was given in table 3. The observed values were also found to have no significant difference to that of the predicted values (p>0.05, Welch's parametric *t*-test for comparing the means). The 3D response surface graphs for the optimization of variables clearly display the investigated results (fig. 8). The values were found satisfactory for the delivery of GTC through the development of GTCTF.
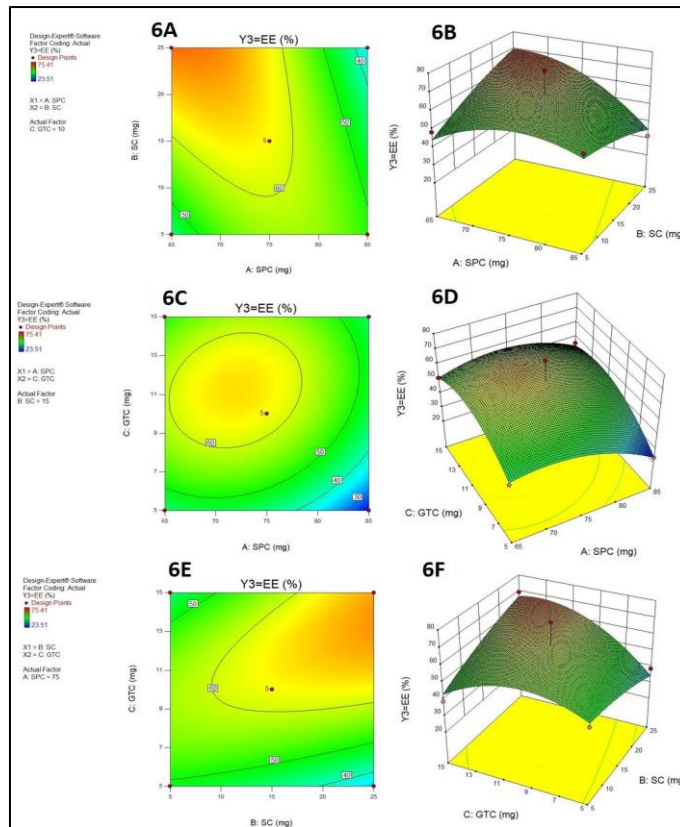
Fig. 6: Contour and Response surface 3D plots showing the effects of the independent variables on EE % (Y3); two independent variables are considered at a time, while the third one remains constant. The variables show a synergistic effect (6B, 6D, 6F) on EE % as represented through the graphs
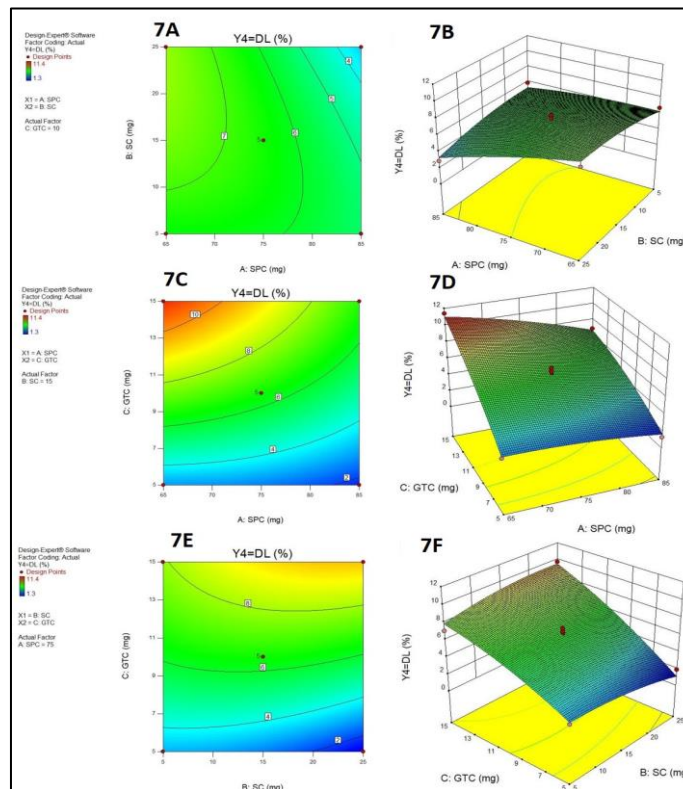

Fig. 7: Contour and response surface 3D plots showing the effects of the independent variables on DL % (Y4); two independent variables are considered at a time, while the third one remains constant. The synergistic effects (7B, 7D, 7F) of the variables on DL % are represented through the graphs

Table 3: Predicted and observed values of optimized GTCTF with its components

Independent variables	Optimized values	
Soya phosphatidylcholine (SPC) (mg)	65	
Sodium cholate (SC) (mg)	25	
Green Tea catechin (GTC) (mg)	15	
Dependent variables or responses	Predicted	Experimental
Particle size (ED) (nm)	168.82±22.27	151.4±1.9*
Polydispersity index (PDI)	0.353±0.015	0.326±0.009*
Entrapment efficiency (EE %)	70.92±7.24	68.25±0.06*
Drug loading (DL %)	12.09±0.73	10.41±0.02*

*Data are given in mean±SD, n=3, *no significant difference between predicted values and experimentally observed values, Welch's parametric *t*-test, p>0.05.
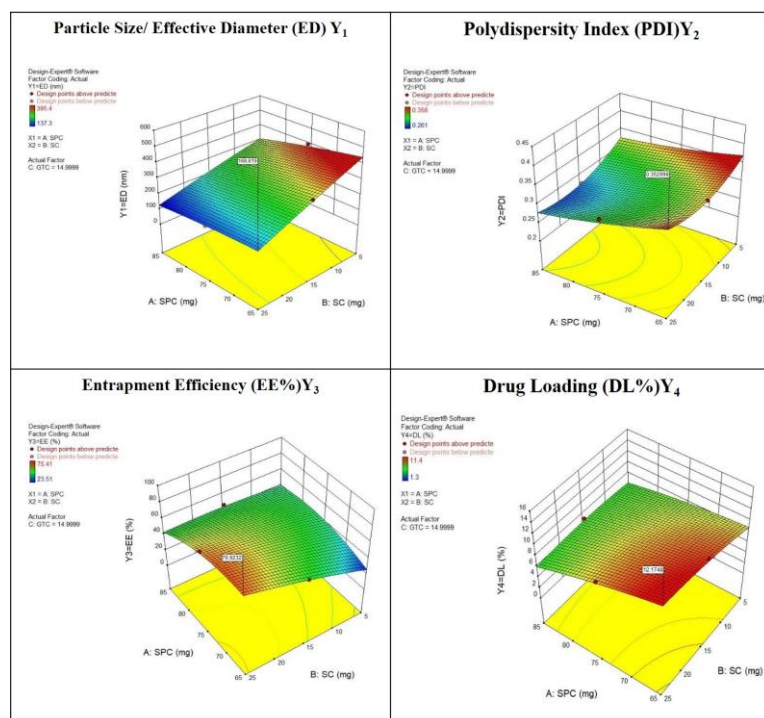
Fig. 8: Response surface 3D plots that show predicted values of the optimized factors A, B, and C. Two independent variables are considered at a time, while the third one remains constant. The predicted values for optimizing the GTCTF components were presented by the graphs

The Box-Behnken response surface design with 3 factors at 3 levels is proven to be a successful statistical method to optimize the transfersomal nanovesicular system incorporating the Green tea catechins extracted from quality green tea. The combined effect of the formulation components was significantly analyzed to get optimum values of the parameters by the BBD model. Statistically optimized nanoformulations are well acceptable to develop nanomedicine for the prevention or treatment of a disease.

Characterization of optimized GTCTFs

Compatibility studies for the components of GTCTF

FT-IR analysis: the characteristic spectrums of SPC, SC, GTC, physical mixture of these three and the lyophilized GTCTF were recorded using FT-IR spectrometer (Alpha, Bruker, Germany. The spectrum was evaluated for characteristic peaks of the samples and changes in the peak (fig. 9) The SPC showed characteristic peaks at 3292.39 cm⁻¹ (O-H stretching), 2921.59 cm⁻¹ (C-H stretching, methylene group), 1735.63 cm⁻¹ (C=O stretching), 1047.93 cm⁻¹(C-N stretching). SC showed its characteristic peaks at 3379.87 cm⁻¹ (O-H stretching), 2928.28 cm⁻¹ (C-H stretching), 1659.02 cm⁻¹ (C=O stretching), 1403.05 cm⁻¹ (O-H bending), 1121.53 cm⁻¹ (C-O stretching). The FT-IR spectrum of GTC showed a board peak at 3235.88 cm⁻¹ (O-H stretch, alcohol), 1601.16 cm⁻¹ (C-O stretching), 1232.32 cm⁻¹ (phenolic C=O stretching), 1037.93 cm⁻¹ (C-O starching).

The FT-IR spectrum of the physical mixture of GTC along with excipients and that of the optimized formulation in lyophilized form revealed the characteristic bands of GTC. These observations indicated the absence of any chemical interactions between the excipients and GTC in the physical mixture as well as in the optimized transfer some formulation.

DSC analysis: DSC is one of the important techniques to explain the physicochemical interaction between the bioactive molecule and excipients of the formulation. Thermodynamic data from DSC analysis is shown in fig. 10. The endothermic peak of GTC was found at 119.92 °C (ΔH = 149.87 J/g), corresponding to the melting points as shown in fig. 10A. The sharp endothermic peak shows the crystalline nature and the anhydrous state of GTC. The DSC thermogram of GTC and its physical mixture with excipients revealed an endothermic peak at 114.7 °C (ΔH = 163.59 J/g) as shown in fig. 10B. The peak intensity was reduced, broadened and slightly shifted, which may be due to the solubilization of GTC in the phospholipid carrier. GTCTF also depicted broadened peak at 132.61 °C (ΔH = 880.29 J/g) with reduced intensity, indicating decreased crystalline nature of GTC and increased drug solubilization in the nanocarrier (fig. 10C). The melting point of GTC was not considerably altered although there was a change in the intensity of the peaks. Hence, the results of DSC analysis suggest the partial amorphization of GTC in the nanocarrier system.
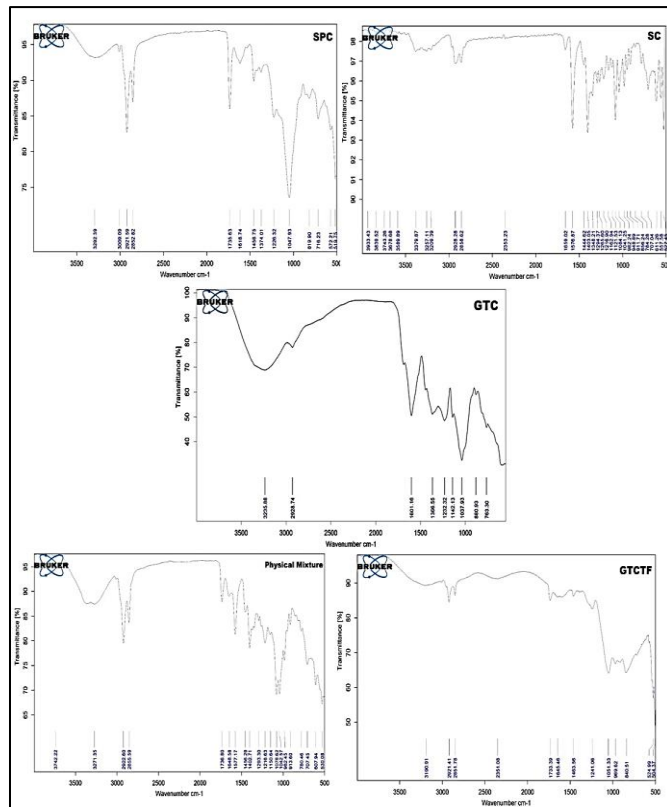
Fig. 9: The FT-IR spectrums of SPC, SC, GTC and their physical mixture and the lyophilized GTCTF. The characteristic peak's position and type of GTC have also been observed in the physical mixture and GTCTF spectra indicating the compatibility between drug and excipients
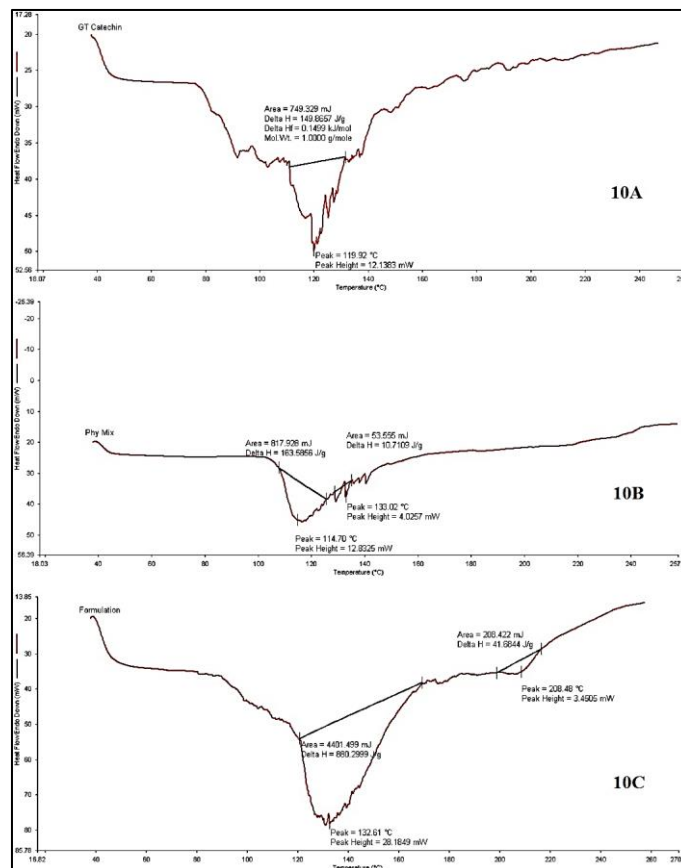

Fig. 10: DSC thermograms of various components. 10A: thermogram of GTC. 10B: thermogram of the physical mixture. 10C: thermogram of GTCTF. The components of GTCTF were found compatible with each other, which indicated successful loading of GTC in transfersomes

Particle size and zeta potential

The particle size of the optimized GTCTF was found 151.4±1.9, PDI 0.326±0.009. The distribution of the size of the GTCTF was found good and in the range of 63.1 to 362.8 nm (fig. 11A). The zeta potential of the GTCTF was measured in Malvern Zeta Sizer and found to be at-11.47±0.46 mV (fig. 11B). Less negative values of zeta potential are helpful in skin permeation and retention of the nanoformulations [60]. The characteristic parameters of the developed GTCTF are displayed in table 4.

High-resolution transmission electron microscopy (HRTEM)

The HRTEM of the GTCTF showed the lipid bilayer vesicular formation of the nanoformulation. The entrapment of the drug to the bilayer core and to the surface of the transfersomes was also observed. The particles are in a satisfactory size range (fig. 11C).

This investigation verifies the successful loading of GTC to the transfersomes.

Entrapment efficiency and drug loading

As discussed earlier, the percentages of entrapment efficiency and drug loading of the optimized formulation were found to be 68.25±0.06 % and 10.41±0.02 %, respectively (table 4). These values verified that the developed GTCTF is a good carrier for the drug GTC to deliver to a targeted site.

Degree of deformability

The degree of deformability of the prepared GTCTF was found to be 18.14±0.02 ml/min (table 4). The vesicles showed to retain their original size after passing through different pore sizes. This confirms the elasticity of the developed transfer some, which is the salient feature of this nanovesicular system [45].
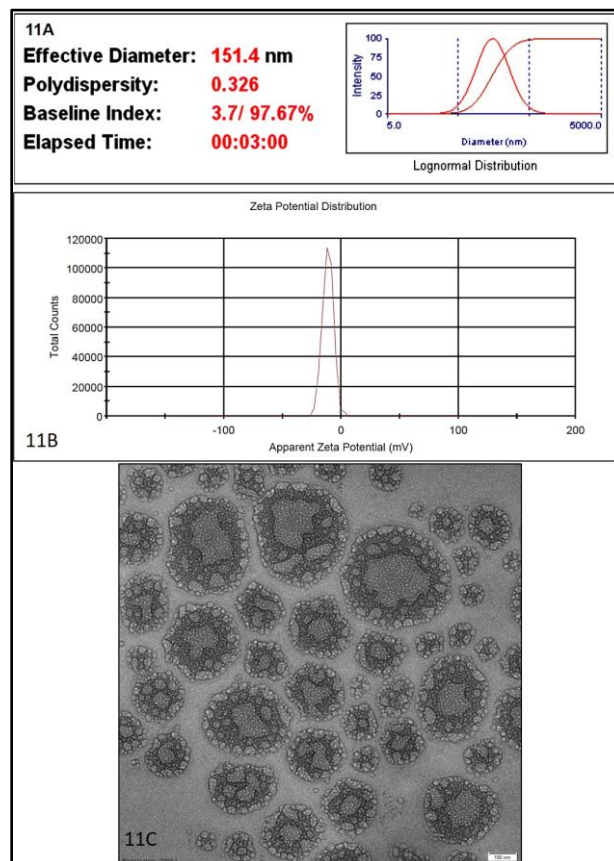

Fig. 11: Physical and morphological evaluation of optimized GTCTF, 11A: Particle size distribution. 11B: Zeta potential distribution graph of GTCTF and the distribution was found acceptable for the optimized GTCTF. 11C: HRTEM image of optimized GTCTF (20000 X magnification) showing vesicular bilayer structure of the optimized GTCTF
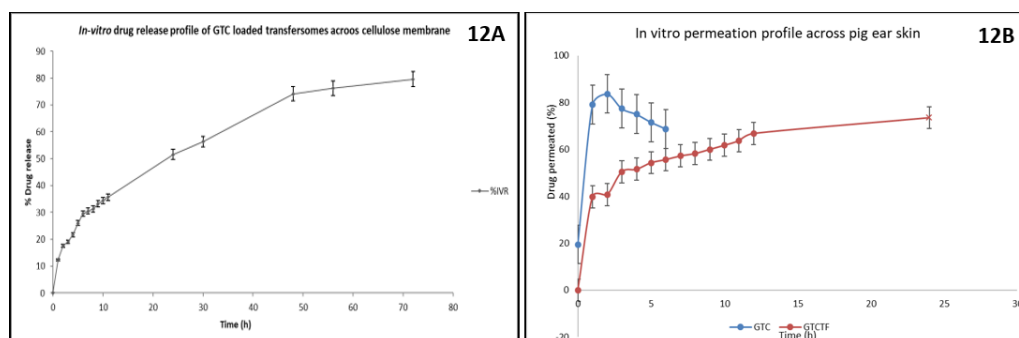

Fig. 12: *In vitro* drug release and permeation profile of GTCTF, 12A: *in vitro* drug release profile of GTC loaded transfersomes across cellulose membrane, 12B: *In vitro* skin permeation profile of GTC and GTCTF. It is clearly observed that GTCTF shows prolonged permeation characteristics through the skin as compared to free GTC, *Data are given in mean±SD, n=3

Table 4: Evaluation of optimized GTCTF

S. No.	Parameters	Results
1	Effective diameter	151.4±1.9 nm
2	PDI	0.326±0.009
3	Entrapment efficiency %	68.25±0.06 %
4	Drug loading %	10.41±0.02 %
5	Zeta potential	-11.47±0.46 mV
6	Deformability index	18.14±0.02 ml/min
7a	Flux (cellulose membrane) J_{ss} GTCTF	7.661±1.69 µg/cm²/h
7b	Flux (Pig Ear Skin) J_{ss} Free GTC	26.37±3.02 µg/cm²/h
7c	Flux (Pig Ear Skin) J_{ss} GTCTF	17.67±0.59 µg/cm²/h

Data are given in mean±SD, n=3

In vitro drug release

In vitro drug release of GTCTF was performed by modified Franz diffusion cell method using cellulose membrane (molecular weight cut-off of 12000 Da). The study shows a maximum drug release of 79.64±3.29 % at 72 h and the Flux (Jss) for GTCTF was found to be 7.661±1.69 µg/cm²/h (fig. 12A and table 4). The prolonged drug release was found satisfactory to controlled, sustained delivery of GTC. The GTCTF is thus capable of slowly releasing the drug to the target site.

In vitro skin permeation study

In vitro skin permeation study of free GTC was performed by a modified Franz diffusion cell method using processed pig ear skin. The study showed immediate permeation of free GTC through pig ear skin, i.e., 83.73±7.29 % at 2 h with Flux (Jss) of 26.37±3.02 µg/cm²/h, after which the release was lowered as the remaining GTC may be impermeable or absorbed by the skin. *In vitro* skin permeation study of GTCTF showed maximum permeation of GTC through the skin at 24 h, i.e., 73.57±1.86 % with Jss of 17.67±0.59 µg/cm²/h. The transfersomes thus have prolonged-release characteristics (fig. 12B and table 4).

Stability of optimized GTCTF

Stability study of the GTCTFs was performed for 6 mo as per ICH guidelines. The transfersomes formulation was stored at 4±1 °C (freeze-stored) and at 25±1 °C with 60±5 % RH (room temperature or RT), separately. Particle size, PDI, and Entrapment efficiency were calculated at monthly intervals for 6 mo. The results are shown in table 5. The freeze-stored GTCTF showed better stability than the RT-stored GTCTF. The GTCTF was found to be stable for 1 mo at RT (table 5). The larger particle size and lower EE % of the GTCTF stored at RT for more than one month may due to the particle agglomeration and leakage of GTC from the transfersomes, respectively.

Table 5: Stability studies of optimized GTCTF for 6 mo

Parameters	0 mo	1 mo		2 mo		3 mo		4 mo		5 mo		6 mo	
		Frz	RT	Frz	RT	Frz	RT	Frz	RT	Frz	RT	Frz	RT
Size (nm)	151.4± 1.9	166.5± 6.3	172.8± 15.1	167.9± 3.4	193.4± 6.2	168.2± 5.1	672.6± 49.9	162.2 ±1.3	758.8 ±99.0	152.7± 3.8	734.4 ±85.0	168.4± 3.2	599.3 ±69.2
PDI	0.326± .009	0.368 ±0.004	0.358 ±0.004	0.362 ±0.003	0.373 ±0.004	0.356 ±0.006	0.405 ±0.045	0.355 ±0.01	0.380 ±0.013	0.346 ±0.007	0.353 ±0.028	0.357 ±0.005	0.367 ±0.003
EE %	68.25± 0.06	67.23± 0.09	66.87± 0.12	66.91± 0.09	65.97 0.09	66.87± .05	59.79± .16	66.73 ±.09	55.93± 0.13	66.51± 0.08	51.58± .15	66.34± .06	49.86± .12

*Data are given in mean±SD, n=3, Frz: freeze-stored, RT: room temperature.
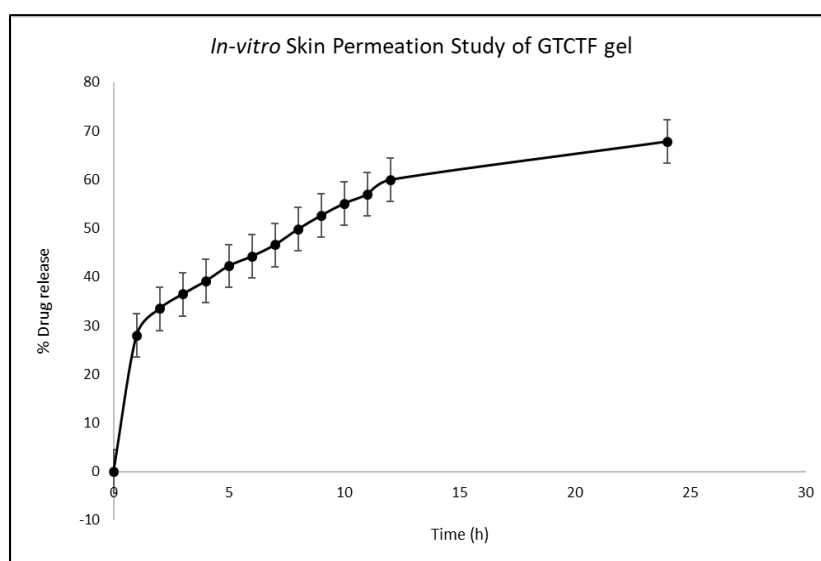

Fig. 13: *In vitro* **skin permeation profile of GTCTF gel across pig ear skin, Data are given in mean±SD, n=3**

Evaluation of developed green tea catechin-loaded transfersomal gel

The gel was prepared by dispersing the optimized GTCTF successfully in a 1.5 % Carbopol 940 gel base and then subjected to further characterization. Transfersomal gel loaded with GTC was assessed for a range of parameters, consistency, homogeneity, clarity, pH, spreadability, drug content and *in vitro* skin permeation. The gel was found to be clear, smooth, homogeneous and spreadable. The distance occupied by transfersomal gel when compressed between slides was used to estimate spreadability. The spreadability of the gel was found to be 1.8±0.1 cm. The pH of the gel was observed to be 5.4±0.2, which was deemed suitable for skin application [49, 50]. The gel's viscosity was measured as $(1.09\pm0.02)\times10^6$cP, indicating that it had enough consistency to be applied to the skin. *In vitro* skin permeation study of GTCTF gel was performed by modified Franz diffusion cell method using processed

pig ear skin. The study showed maximum permeation of GTC through the skin at 24 h i.e., 67.78±0.89 % (fig. 13). The transfersomes gel thus has prolonged-release characteristics than free GTCTF, facilitating controlled delivery of the nanoformulations owing to the incorporation of the GTCTF in gel matrix.

***In vitro* anticancer activity**

The *in vitro* anticancer activity of the optimized GTCTF was evaluated using MTT (3-(4, 5-dimethylthiazol-2-yl)-2, 5-diphenyltetrazolium bromide) assay on B6F10 cell lines. IC 50 values for 5-FU, GTCTF (concentration equivalent to the entrapped drug was considered) and free GTC were found to be 79.85 µg/ml, 199.10 µg/ml and 460.10 µg/ml, respectively (fig. 14A). The % cell viability of the samples was represented in fig. 14B. The % cell viability and IC_{50} of GTCTF were found better than free GTC. The results also confirm the cytotoxicity of GTCTF as compared to the standard anticancer drug 5-FU.
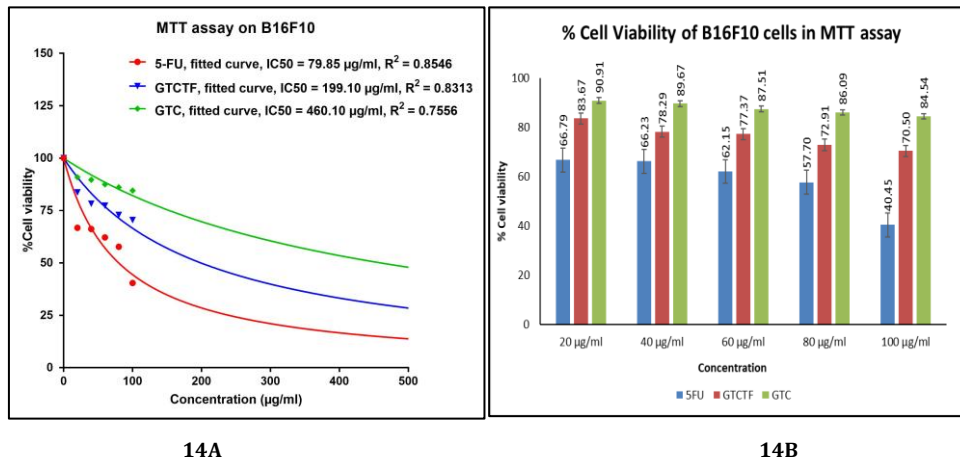
14A **14B**

Fig. 14: Graphs showing results of MTT assay on B16F10 cell lines, 14A: Inhibitor (concentration) vs normalized response (% cell viability) for non-linear curve fitting using GraphPad Prism V7 for IC_{50} value evaluation for GTCTF, 5-FU and GTC. 14B: % cell viabilities of 5-FU, GTC, and GTCTF at different concentrations. GTCTF was found cytotoxic to B16F10, similar to 5-FU (not significantly different p>0.05, Welch's t-test, unpaired and parametric), Data are given in mean, n=3

Skin irritation study

The skin irritation study for the GTCTF gel was performed on rabbit dorsal skin. The GTCTF equivalent to 0.5 g was applied on the dorsal

(hair-removed) skin of the rabbit at a single dose. The animals were observed for 7 d. No edema, no erythema was observed in the skin. The GTCTF gel was established to be safe for topical application (fig. 15).

Fig. 15: Skin irritation study of GTCTF on rabbits, 15A: Dorsal skin of rabbit treated with blank gel showing no irritation. 15B: Dorsal skin of rabbit treated with GTCTF gel showing no irritation

***In vivo* chemopreventive and anticancer activity of GTCTF gel**

Chemopreventive activity

In the chemopreventive activity experiment, the GTCTF gel was applied to the Group VI animals along with the carcinogen DMBA to

investigate how much GTCTF can prevent the formation of tumor or cancer on the skin. Group V treated with only DMBA has shown the induction of cancer at the 10th w. After induction, animals were left without drug administration for 4 more w to develop or spread cancer. It was found that the cancer induction in the GTCTF pretreated group

is very less as compared to the cancer control group. After 14th w the animals were sacrificed to collect skin for biochemical and histopathology study. The biochemical study for estimation of cancer-specific markers TNFα, IL-6 and IL-1β was done by using the ELISA method from the tissue lysate samples. The result showed lower levels of these markers in the GTCTF gel pretreated group (fig. 16 and table 6). The histopathological study confirms that the GTCTF gel treated group showed almost normal skin structure with mild to moderate

prevention of skin carcinogenesis and architecture but with a little hyperkeratosis, inhibition of dermal cell proliferation was also observed (fig. 17C). The cancer control group showed epithelial, vascular lesion, epidermal hyperplasia with hyperkeratosis, tumor nest, and parakeratosis. The skin was illustrated by thickening of the epidermis, epidermal cells invasion into the dermis, and hyperkeratosis (fig. 17B). The results confirm the chemopreventive action of GTCTF gel on the experimental animal model.
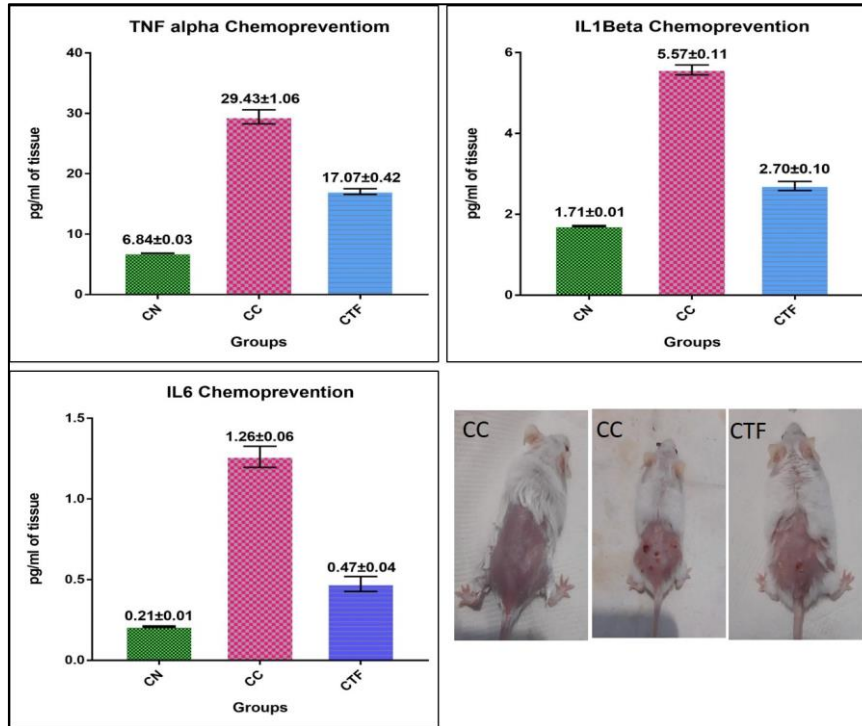

Fig. 16: Biochemical evaluation for chemopreventive nature of GTCTF, CN=Normal Group, CC=Cancer control group, CTF= GTCTF treated group. The biochemical analysis was performed using ELISA kit. GTCTF successfully reduced the TNFα, IL-6 and IL-1β levels in the skin tissue, indicating its chemopreventive nature. The respective mice images before collecting skin tissues are also displayed in this fig., Data are given in mean±SD, n=6
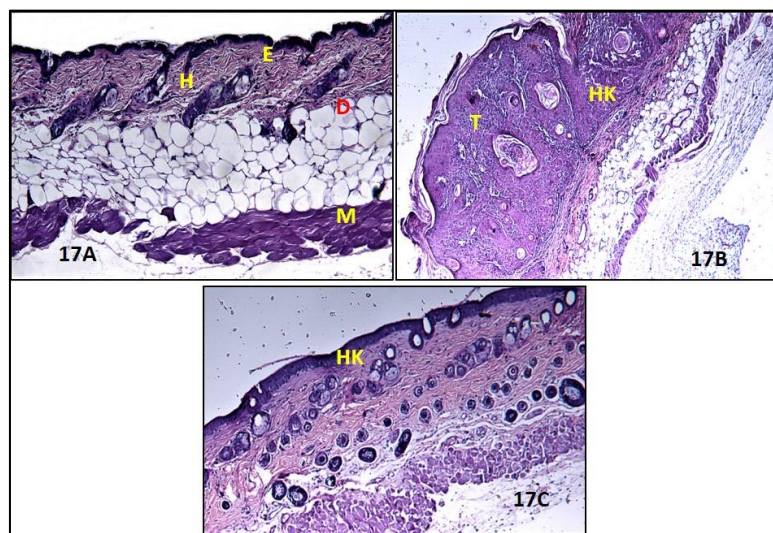

Fig. 17: Histopathology study for the chemopreventive activity of GTCTF (Hematoxylin and eosin stained skin samples), 17A: The skin of control mice treated with the vehicle shows a normal distribution of the different skin layers. Hair follicles (H), Epidermis (E), dermis (D), muscle fibers (M) are well structured. 17B: The cancer controls group showed epithelial, vascular lesion, epidermal hyperplasia with hyperkeratosis (HK) and tumor nest (T). The skin was illustrated by thickening of the epidermis, epidermal cells invasion into the dermis. 17C: GTCTF gel treated group showed almost normal skin structure mild to moderate prevention of skin carcinogenesis and architecture but with a little hyperkeratosis; inhibition of dermal cell proliferation was also noticed

Table 6: Levels of biochemical parameters found on skin tissue sample using ELISA

Parameters	Anti-skin cancer activity				Chemopreventive activity		
	TN[#1]	TC[#1]	TFU[#1]	TTF[#1]	CN[#2]	CC[#2]	CTF[#2]
TNFα	6.73±0.15	28.84±1.48*	14.06±1.05	16.56±1.35[a]	6.84±0.03	29.43±1.06	17.07±0.42[b]
IL-1β	1.78±0.11	5.03±0.34*	2.25±0.18	2.75±0.16[a]	1.71±0.01	5.57±0.11	2.70±0.10[b]
IL-6	0.17±0.02	1.08±0.18*	0.37±0.05	0.44±0.05[a]	0.21±0.01	1.26±0.06	0.47±0.04[b]

Data are given in mean±SD, n=6, unit of the data is pg/mg of tissue. [#1]values are significant, $p<0.05$, one-way ANOVA, among the anti-skin cancer groups. [#2]values are significant, $p<0.05$, one-way ANOVA among the chemopreventive groups. *values are significant, TC compared to TN. two-tailed Unpaired t-test, $p<0.0001$. [a]values are significant. TTF compared to TC, two-tailed unpaired t-test, $p<0.001$. [b]values are significant, CTF compared to CC, two-tailed unpaired t-test, $p<0.001$.

Anti-skin cancer activity

The anti-skin cancer activity differs from the chemoprevention in the criteria that in the anticancer model the treatment was introduced after the complete and confirm induction of cancer or tumor to the skin. In this study, four groups of animals were used each including 3 mice. Group I (TN) was treated with a 1.5 % Carbopol 940 gel base only used to refer to normal skin structure and tissue biochemical parameters. Group II (CC) was treated with DMBA and acted as a Cancer Control group. Group III (TFU) received the established anti-skin cancer formulation Flonida (1% 5-FU topical gel) as a reference standard. The last Group VI (TTF) was administered with a developed 3 % GTCTF gel. Animals of Group II to IV were administered with DMBA to induce cancer. It was observed that it took 10th w to induce skin cancer in the treated animals with the application of DMBA. Treatments were started after the induction of skin cancer, while DMBA was being applied up to the 14th w and then stopped. The treatment was carried out for 22nd w when observations were found satisfactory with a reduced number of tumor numbers and size and returning the normal skin texture and hair growth in the treatment groups. At the end of the 22nd w, animals were sacrificed and skin samples were collected for histopathological and biochemical investigation.

The skin slides of Group II have illustrated the occurrence of hyperplasia, epidermal cells with cellular atypia. Irregularly increased thickness of non-keratinized layers (K) of the epidermis with partial loss of normal differentiation was noticed. Well-circumscribed mass composed of uniform lobules (L) of closely packed basaloid cells were observed (fig. 18B1). Tumor cells form circumscribed nests with central necrosis (N). The slide showed foci of microcarcinoma as groups of epidermal cells deepening in the dermis. Increased size of epidermal keratinocytes (EK) with cytoplasmic pallor and displacement of the nucleus to the periphery of the cell was also observed (fig. 18B2).

The slides of skin samples from the Flonida 1% treated group showed normal skin structure with mild to moderate recovery of skin carcinogenesis but with hyperkeratosis, inhibition of dermal cell proliferation, follicular epithelial hyperplasia (F) (fig. 18C). Similarly, in the skin samples from the GTCTF gel treated animals it was observed that it has almost normal skin structure with mild to the moderate recovery of skin carcinogenesis and architecture but with a mild hyperkeratosis(K), mild multifocal hyperplasia (M), minimal dermatitis and fibrosis, inhibition of dermal cell proliferation (ID), increase in dermal cell differentiation (fig. 18D).
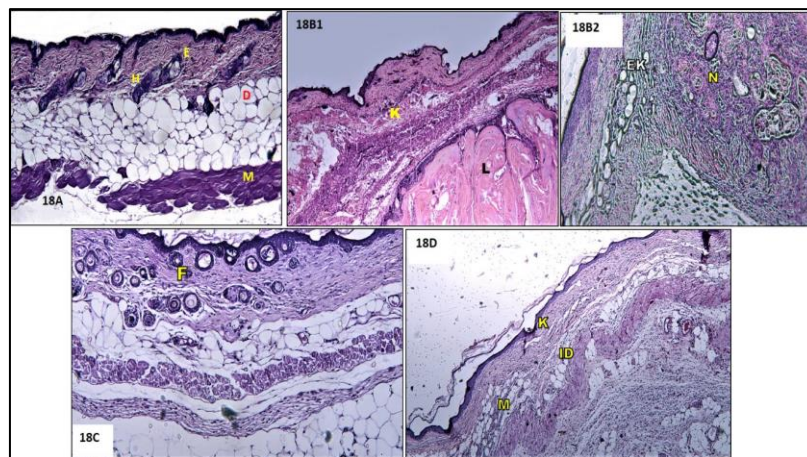
Fig. 18: Histopathology study for anticancer activity of GTCTF (hematoxylin and eosin stained skin samples), 18A: The skin of control mice treated with the vehicle shows a normal distribution of the different skin layers. Hair follicles (H), Epidermis (E), dermis (D), and muscle fibers (M) are well structured. 18B1-18B2: Cancer control group showing Hyperplasia, epidermal with cellular atypia. Irregularly increased thickness of non-keratinized layers (K) of the epidermis with partial loss of normal differentiation Well circumscribed mass composed of uniform lobules (L) of closely packed basaloid cells. Tumor cells form circumscribed nests with central necrosis (N). Foci of microcarcinoma as groups of epidermal cells deepening in the dermis. Increased size of epidermal keratinocytes (EK) with cytoplasmic pallor and displacement of the nucleus to the periphery of the cell. 18C: Flonida 1% treated groups showing normal skin structure with mild to moderate recovery of skin carcinogenesis but with hyperkeratosis, inhibition of dermal cell proliferation, follicular epithelial hyperplasia (F). 18D: GTCTF gel treated groups showing normal skin structure with mild to the moderate recovery of skin carcinogenesis and architecture but with a mild hyperkeratosis (K), mild multifocal hyperplasia (M), minimal dermatitis and fibrosis, inhibition of dermal cell proliferation (ID), increase in dermal cell differentiation

From the biochemical investigation of cancer markers in the tissue, it was observed that the levels of TNFα, IL-6, and IL-1β were highly elevated in the animals of the cancer control group than in the normal animals significantly. Whereas their levels are significantly lowered in the marketed formulation and GTCTF gel treated group than in the cancer control group. The developed gel showed a similar anticancer effect to the marketed one (fig. 19 and table 6).
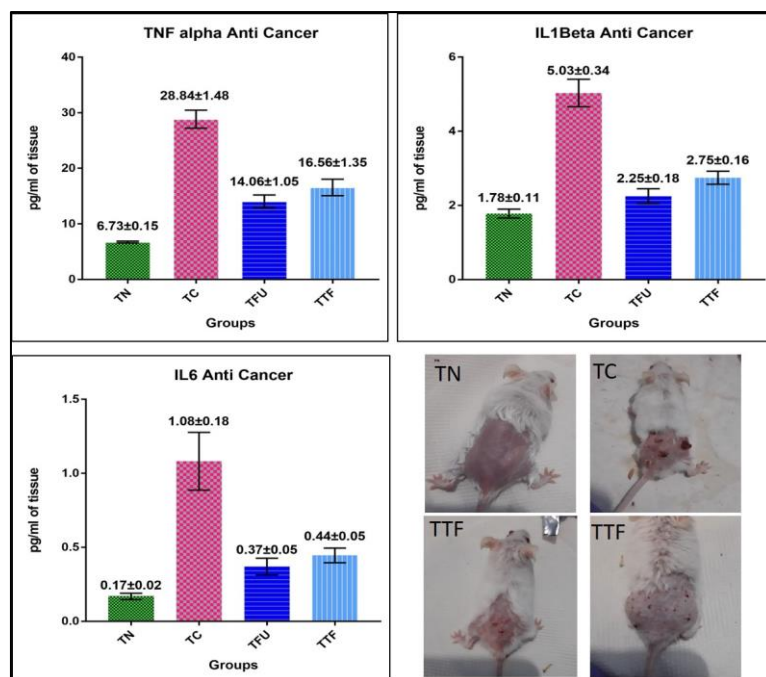
Fig. 19: Biochemical evaluation for anticancer nature of GTCTF, CN=Normal Group, CC=Cancer control group, CTF= GTCTF treated group. The biochemical analysis was performed using a specific ELISA kit for tissue lysate. GTCTF successfully reduced the TNFα, IL-6 and IL-1β levels in the skin tissue, indicating its anticancer nature, The respective mice images before collecting skin tissues are also displayed in this fig., *Data are given in mean±SD, n=6

DISCUSSION

Among the types of cancer, skin cancer in recent year have been found to increase in numbers in India and globally as well [6-8]. To replace the limitations like pain, skin irritation, rashes, and psoriasis, of the conventional treatment and prevention techniques, a novel approach to utilizing an herbal drug obtained from highly consumed green tea has been investigated in this study. Unlike isolated single compounds, a mixture of anticancer components in a single herbal drug is always been a cost-effective approach [15-24]. Assam is known for the world's best quality of green tea. With so much biodiversity and availability at fingertips, the green tea catechin extract (GTC) collected from locally produced and marketed green tea leaves have been used as an herbal drug after standardization in the current study. This was the very basic novel approach to utilizing the vast available resources in our motherland in search of benefits for public health and well-being.

The extraction of the GTC from green tea leaves by the hot aqueous infusion method followed by separation with chloroform and ethyl acetate was found satisfactory, with an acceptable yield and removal of caffeine. The standardization of the extracted GTC with reference to the pure components of catechin showed that the extraction method and the idea of utilizing local resources as the herbal drug could be effective and fruitful. The extracted GTC has similar characteristic peaks and bands in UV-Vis and FT-IR spectrum and HPTLC chromatography as compared to Standard Polyphenon 60 and EGCG (fig. 1 to fig. 3), which assured that the GTC extract has required pharmacologically active ingredients. To successfully deliver the drug, a good carrier is always mandatory for a controlled and targeted drug delivery approach [9-12].

To use GTC against skin cancer, the nano vesicular system of transfersomes containing soya phosphatidylcholine as phospholipid and sodium cholate as edge activator was developed using statistical Box-Behnken design for optimization. A statistically optimized nanoformulation is always considered as an acceptable and effective potential drug delivery approach [41]. The Box-Behnken response surface design for optimization with the point prediction method for optimization was successfully applied in the current study. The important characteristic parameters of a nanoformulation like particle

size, PDI, drug entrapment efficiency, and drug loading were significantly optimized with the use of the predicted amounts of GTCTFs components by using this model approach (table 2 and table 3). All four responses, particle size (Eq. 5), PDI (Eq. 6), EE % (Eq. 7), DL % (Eq. 8), were found to be significantly fitted to the quadratic model with respect to the independent variables. The combined effects of the transfersomal components were illustrated by the contour and the 3D graphs. The synergistic effect of SPC and GTC, and the antagonistic effect of SC on vesicle size were presented in fig. 4. In fig. 5, the synergistic effect of SC and GTC, and the antagonistic effect of SPC on PDI were shown. Similarly, the synergistic effects of all the variables of EE % and DL % were thoroughly illustrated in fig. 6 and fig. 7, respectively. It was observed that a direct increase or decrease of the amount of the components not always changes the responses proportionally. A high amount of SPC and SC results in the formation of smaller vesicles with low EE % (F2, table 2). This may be due to the increased permeability of the transpersonal membrane, where arrangements of the surfactant molecules in the lipid bilayer enhance fluidity and evoke leakage of the drug [61]. Low SPC and high SC content have prompted an acceptable vesicle size and EE % (F7, table 2). Similarly, a high amount of drug in transfersome produced vesicles with high EE % (F16, table 2). The point prediction and confirmation method verified that the results of responses evaluated for the optimized GTCTF were similar to the predicted values for the same. The Box-Behnken design was established to be an acceptable statistical approach for the optimization of the nanoformulation.

The compatibility studies showed that there were no possible changes in the structure and nature of the components of GTCTF. The FT-IR spectrum of the physical mixture and the formulation suggested the presence of a characteristic broad peak of O-H bond of GTC unchanged (fig. 9). Similarly, in the DSC thermogram, it was observed that the endothermic peaks for GTC were present in the same position in the physical mixture and the GTCTF formulation (fig. 10). The little change in nature of crystallinity was acceptable which may be due to encapsulation or solubilization of the drug to the phospholipid bilayer of the transfersomes. The presence of all the characteristic peaks of each component in their physical mixture and GTCTF confirms their compatibility with each other and no chemical reaction within themselves [62, 63].

163

The characterization of the developed optimized GTCTF describes that it was a very suitable nanovesicular system for delivery of GTC to the skin. The zeta potential with a low negative charge could be useful for potential skin delivery of GTC [58]. The deformability studies implied that the prepared GTCTF has the basic criteria of a transfersome i.e., it can squeeze out through a range of pores by retaining its original shape and size after permeation [43, 44]. *In vitro* drug release and skin permeation studies to get the time for maximum release were carried out to evaluate the controlled release aspects of GTCTF for which they were meant to develop. The vitro drug release study showed slow release of GTC from the GTCTF, which was due to the encapsulation of GTC in the lipid bilayer of transfersomes that act as a barrier for the fast release associated with free GTC [64] and may be due to very small pore size ($\sim$ 2.9 nm for 10 kDa) of the cellulose membrane [65]. However, the release of GTCTF, through such pores that were very much smaller than GTCTF's size has supported the deformability and squeezing-out capacity of developed transfersomes [62, 63]. The skin permeation study verified that the developed GTCTF was more suitable to attain a prolonged controlled release profile than free GTC, which could facilitate the drug to be in the skin layer for a longer period of time for the management of skin cancer. The GTCTF was found to be stable at refrigerated temperature for up to six months, whereas it was stable at room temperature for a period of one month. At room temperature, the particle size has been observed to increase and the entrapped drug was found to be released after one month. This may be due to agglomeration and swelling of the particles or breakdown of the bilayer structure and leakage of drugs from the vesicles.

The *in vitro* anticancer study on B16F10 murine skin cancer cells suggests that the optimized GTCTF has acceptable anticancer activity. Although the activity was low compared to 5-FU, this might be helpful for contributing fewer side effects to its topical use. The % cell viability of free GTC was observed to be very less or uncountable. GTCTF showed an appreciable cytotoxic effect on the cancer cells (fig. 14). A higher concentration of GTCTF could be used to attain the desired anticancer effect.

After complete characterization, it was important to develop a vehicle of nanomedicine for skin delivery. In the current study, we had developed Carbopol 940 (1.5 %w/w) gel for the delivery of GTCTF. The *in vitro* anticancer study results were considered to prepare an effective dose of the GTCTF. In this study, we used GTCTF equivalent to 3 % w/w GTC to prepare the topical gel. The gel was found to be smooth, homogenous and consistent. The pH of 5.4 was very acceptable for topical application. The viscosity and spreadability of the prepared gel were found to be suitable for topical application. Moreover, the *in vitro* skin permeation study of GTCTF gel has evinced the prolonged release of GTC even more than that of free GTCTF (fig. 13) [51, 54].

The safety of the prepared GTCTF gel for topical use was accessed by using the OECD skin irritation study guideline (No. 404). The use of the topical gel on the skin of rabbits showed no edema or erythema or any other irritation to the skin as observed in fig. 15. The GTCTF gel was safe to be used for topical administration.

The developed GTCTF gel was found to possess acceptable and effective *in vivo* chemopreventive and anti-skin cancer activity in the experimental animal model. The GTCTF gel successfully prevents skin cancer when applied as pretreatment and simultaneously along with the carcinogen to the skins of the animals. It was also proved to have a suitable anticancer activity against DMBA-induced skin cancer. Histological studies of the skin samples have confirmed the preventive (fig. 17) and anticancer effects (fig. 18) of the GTCTF against skin cancer. These results were further confirmed by biochemical analysis of the skin tissues, where TNFα, IL-6, and IL-1β were reduced significantly in the treatment groups (fig. 16 and fig. 19). Chronic inflammation is considered a major driving force for skin carcinogenesis. TNF-α, IL-6, and IL-1β appear to be the major components of cancer-associated cytokine networks, usually resulting in cytokine-associated inflammation in cancer [66-68]. Lowering the elevated levels of these markers supports the anticancer and chemopreventive effects of GTCTF gel.

The findings from the current study strongly established that the developed green tea catechin-loaded transfersomes (GTCTF) have both chemopreventive and anticancer activity against DMBA-induced skin cancer in mice. Box-Behnken statistical design was found effective in developing an optimized GTCTF. The results showed the goal of the study to manage skin cancer with GTCTF was successful. The GTCTF gel showed desired cancer management effect as compared to the marketed 5-FU formulation for skin cancer treatment. However, it can be predicted that prolonged use of GTCTF gel may completely recover from the skin damage caused due to skin cancer.

CONCLUSION

In the current study, green tea catechins were successfully extracted from green tea leaves obtained from Assam, India. The statistical Box Behnken design approach to develop an optimized nanovesicular formulation i.e., transfersome, loaded with GTC was proved to be a promising tool. The components of the nanovesicular formulation of GTC were fixed in such a way that it gave smaller nanovesicles with higher drug entrapment efficiency and drug loading for favorable skin delivery of GTC against skin cancer. The MTT assay of the GTCTF was found satisfactory for its cytotoxic effect against B16F10 skin cancer cell lines. The developed Carbopol 940 gel of the GTCTF has desirable characteristics like pH, viscosity, spreadability, and permeability for topical application. The GTCTF gel was also found to be safe for topical application. The nanovesicular herbal gel showed promising cancer management in the *in vivo* experimental animal model. Further, the comparison of the biochemical markers of the skin tissues has strongly supported the anti-skin cancer effect of the nanovesicular system of green tea catechin. However, further studies are warranted for the development of clinically effective topical gel in the management of skin cancer.

INSTITUTIONAL REVIEW BOARD STATEMENT

The protocol for general procedures and use of animals for conducting this study has been reviewed and approved by the Institutional Animal Ethics Committee, Department of Pharmaceutical Sciences, Dibrugarh University (Approval No. IAEC/DU/156 dated 01/11/2018) and was performed according to the committee's guidelines for the use of laboratory animals.

AUTHORS CONTRIBUTIONS

Conceptualization, Das MK and Deka T; methodology, Deka T and Das MK; software, Deka T; formal analysis, Deka T; investigation, Deka T and Das S; data curation, Deka T; validation, Deka T and Das MK; writing-original draft preparation, Deka T; writing-review and editing, Das MK, Das S, Das P and Singha LR; supervision, Das MK; project administration, Das MK.; funding acquisition, Das MK and Deka T. All authors have read and agreed to the published version of the manuscript.

CONFLICT OF INTERESTS

We declare that we have no conflict of interest.

REFERENCES

1. Jones OT, Ranmuthu CKI, Hall PN, Funston G, Walter FM. Recognising skin cancer in primary care. Adv Ther. 2020;37(1):603-16. doi: 10.1007/s12325-019-01130-1, PMID 31734824.

2. Bradford PT. Skin cancer in skin of color. Dermatol Nurs. 2009;21(4):170-8. PMID 19691228.

3. Apalla Z, Lallas A, Sotiriou E, Lazaridou E, Ioannides D. Epidemiological trends in skin cancer. Dermatol Pract Concept. 2017;7(2):1-6. doi: 10.5826/dpc.0702a01, PMID 28515985.

4. Linares MA, Zakaria A, Nizran P. Skin cancer. Prim Care. 2015;42(4):645-59. doi: 10.1016/j.pop.2015.07.006, PMID 26612377.

5. Saginala K, Barsouk A, Aluru JS, Rawla P, Barsouk A. Epidemiology of melanoma. Med Sci (Basel). 2021;9(4):63. doi: 10.3390/medsci9040063, PMID 34698235.

6. Perera E, Gnaneswaran N, Staines C, Win AK, Sinclair R. Incidence and prevalence of non-melanoma skin cancer in Australia: a systematic review. Australas J Dermatol. 2015;56(4):258-67. doi: 10.1111/ajd.12282, PMID 25716064.

7. Labani S, Asthana S, Rathore K, Sardana K. Incidence of melanoma and nonmelanoma skin cancers in Indian and the global regions. J Cancer Res Ther. 2021;17(4):906-11. doi: 10.4103/jcrt.JCRT_785_19, PMID 34528540.

8. India Population Fact Sheet. WHO International Agency for Cancer Research. Available from: https://gco.iarc.fr/today/ data/factsheets/populations/356-india-fact-sheets.pdf. [Last accessed on 02 Mar 2022].

9. Priya P, Mohan Raj RM, Vasanthakumar V, Raj V. Curcumin-loaded layer-by-layer folic acid and casein coated carboxymethyl cellulose/casein nanogels for treatment of skin cancer. Arab J Chem. 2020;13(1):694-708. doi: 10.1016/j.arabjc.2017.07.010.

10. Shukla T, Upmanyu N, Agrawal M, Saraf S, Saraf S, Alexander A. Biomedical applications of microemulsion through dermal and transdermal route. Biomed Pharmacother. 2018;108:1477-94. doi: 10.1016/j.biopha.2018.10.021, PMID 30372850.

11. Iqbal J, Abbasi BA, Ahmad R, Batool R, Mahmood T, Ali B. Potential phytochemicals in the fight against skin cancer: current landscape and future perspectives. Biomed Pharmacother. 2019;109:1381-93. doi: 10.1016/ j.biopha.2018.10.107, PMID 30551389.

12. Chinembiri TN, du Plessis LH, Gerber M, Hamman JH, du Plessis J. Review of natural compounds for potential skin cancer treatment. Molecules. 2014;19(8):11679-721. doi: 10.3390/ molecules190811679, PMID 25102117.

13. Bhutadiya VL, Mistry KN. A review on bioactive phytochemicals and it's mechanism on cancer treatment and prevention by targeting multiple cellular signaling pathways. Int J Pharm Pharm Sci. 2021;13:15-9. doi: 10.22159/ijpps.2021v13i12.42798.

14. Ng CY, Yen H, Hsiao HY, Su SC. Phytochemicals in skin cancer prevention and treatment: an updated review. Int J Mol Sci. 2018;19(4):941. doi: 10.3390/ijms19040941, PMID 29565284.

15. Cheng Z, Zhang Z, Han Y, Wang J, Wang Y, Chen X. A review on the anti-cancer effect of green tea catechins. J Funct Foods. 2020;74:104172. doi: 10.1016/j.jff.2020.104172.

16. Mittal A, Piyathilake C, Hara Y, Katiyar SK. Exceptionally high protection of photocarcinogenesis by topical application of (-)-epigallocatechin-3-gallate in hydrophilic cream in SKH-1 hairless mouse model: relationship to inhibition of UVB-induced global DNA hypomethylation. Neoplasia. 2003;5(6):555-65. doi: 10.1016/s1476-5586(03)80039-8, PMID 14965448.

17. Magcwebeba TU, Riedel S, Swanevelder S, Swart P, De Beer D, Joubert E. The potential role of polyphenols in the modulation of skin cell viability by *Aspalathus linearis* and cyclopia spp. Herbal tea extracts *in vitro*. J Pharm Pharmacol. 2016;68(11):1440-53. doi: 10.1111/jphp.12629, PMID 27671741.

18. Katiyar SK, Mohan RR, Agarwal R, Mukhtar H. Protection against induction of mouse skin papillomas with low and high risk of conversion to malignancy by green tea polyphenols. Carcinogenesis. 1997;18(3):497-502. doi: 10.1093/carcin/ 18.3.497, PMID 9067548.

19. Przystupski D, Michel O, Rossowska J, Kwiatkowski S, Saczko J, Kulbacka J. The modulatory effect of green tea catechin on drug resistance in human ovarian cancer cells. Med Chem Res. 2019;28(5):657-67. doi: 10.1007/s00044-019-02324-6.

20. Manikandan R, Beulaja M, Arulvasu C, Sellamuthu S, Dinesh D, Prabhu D. Synergistic anticancer activity of curcumin and catechin: an *in vitro* study using human cancer cell lines.

21. Microsc Res Tech. 2012;75(2):112-6. doi: 10.1002/jemt.21032, PMID 21780253.

21. Braicu C, Gherman CD, Irimie A, Berindan Neagoe I. Epigallocatechin-3-gallate (EGCG) inhibits cell proliferation and migratory behaviour of triple-negative breast cancer cells. J Nanosci Nanotechnol. 2013;13(1):632-7. doi: 10.1166/jnn.2013.6882, PMID 23646788.

22. Shim JH, Su ZY, Chae JI, Kim DJ, Zhu F, Ma WY. Epigallocatechin gallate suppresses lung cancer cell growth through Ras-GTPase-activating protein SH3 domain-binding protein 1. Cancer Prev Res (Phila). 2010;3(5):670-9. doi: 10.1158/1940-6207.CAPR-09-0185, PMID 20424128.

23. Tyagi T, Garlapati PK, Yadav P, Naika M, Mallya A, Kandangath Raghavan A. Development of nano-encapsulated green tea catechins: studies on optimization, characterization, release dynamics, and *in vitro* toxicity. J Food Biochem. 2021;45(11):e13951. doi: 10.1111/jfbc.13951, PMID 34569069.

24. PM, V BB, KN CM, NA, SB. Enrichment of *in vivo* efficacy of catechin-rich extract with the application of nanotechnology. Int J Appl Pharm. 2018;10(5):281-8. doi: 10.22159/ijap.2018v10i5.29569.

25. Krishnan V, Mitragotri S. Nanoparticles for topical drug delivery: potential for skin cancer treatment. Adv Drug Deliv Rev. 2020;153:87-108. doi: 10.1016/j.addr.2020.05.011, PMID 32497707.

26. Natarajan SB, Chandran SP, Vinukonda A, Rajan DS. Green tea catechin loaded nano delivery systems for the treatment of pandemic diseases. Asian J Pharm Clin Res. 2019;12(5):1-7.

27. Chen J, Shao R, Zhang XD, Chen C. Applications of nanotechnology for melanoma treatment, diagnosis, and theranostics. Int J Nanomedicine. 2013;8:2677-88. doi: 10.2147/IJN.S45429, PMID 23926430.

28. Tsai YJ, Chen BH. Preparation of catechin extracts and nanoemulsions from green tea leaf waste and their inhibition effect on prostate cancer cell PC-3. Int J Nanomedicine. 2016;11:1907-26. doi: 10.2147/IJN.S103759, PMID 27226712.

29. Chen CC, Hsieh DS, Huang KJ, Chan YL, Hong PD, Yeh MK. Improving anticancer efficacy of (-)-epigallocatechin-3-gallate gold nanoparticles in murine B16F10 melanoma cells. Drug Des Dev Ther. 2014;8:459-74. doi: 10.2147/DDDT.S58414, PMID 24855338.

30. Jiang Y, Jiang Z, Ma L, Huang Q. Advances in nanodelivery of green tea catechins to enhance the anticancer activity. Molecules. 2021;26(11):3301. doi: 10.3390/ molecules26113301, PMID 34072700.

31. Harwansh RK, Mukherjee PK, Kar A, Bahadur S, Al-Dhabi NA, Duraipandiyan V. Enhancement of photoprotection potential of catechin loaded nanoemulsion gel against UVA-induced oxidative stress. J Photochem Photobiol B. 2016;160:318-29. doi: 10.1016/j.jphotobiol.2016.03.026, PMID 27167597.

32. Abd El-Alim SH, Kassem AA, Basha M, Salama A. Comparative study of liposomes, ethosomes and transfersomes as carriers for enhancing the transdermal delivery of diflunisal: *in vitro* and *in vivo* evaluation. Int J Pharm. 2019;563:293-303. doi: 10.1016/j.ijpharm.2019.04.001, PMID 30951860.

33. Shaji J, Garude S. Transethosomes and ethosomes for enhanced transdermal delivery of ketorolac tromethamine: a comparative assessment. Int J Curr Pharm Res. 2014;6:88-93.

34. Abdel-Hafez SM, Hathout RM, Sammour OA. Curcumin-loaded ultra deformable nanovesicles as a potential delivery system for breast cancer therapy. Colloids Surf B Biointerfaces. 2018;167:63-72. doi: 10.1016/j.colsurfb.2018.03.051, PMID 29626721.

35. Cevc G, Blume G. New, Highly efficient formulation of diclofenac for the topical, transdermal administration in ultradeformable drug carriers, transfersomes. Biochim Biophys Acta. 2001;1514(2):191-205. doi: 10.1016/s0005-2736(01)00369-8, PMID 11557020.

36. Fujiki H, Sueoka E, Watanabe T, Suganuma M. Synergistic enhancement of anticancer effects on numerous human cancer cell lines treated with the combination of EGCG, other green tea catechins, and anticancer compounds. J Cancer Res Clin Oncol. 2015;141(9):1511-22. doi: 10.1007/s00432-014-1899-5, PMID 25544670.

37. Bharaduwaj M, Das MK. Preformulation optimization of catechin extracts from assam green tea as a candidate for topical chemoprevention. World J Pharm Res. 2018;7:1035-48.
38. Row KH, Jin Y. Recovery of catechin compounds from Korean tea by solvent extraction. Bioresour Technol. 2006;97(5):790-3. doi: 10.1016/j.biortech.2005.04.001, PMID 15919205.
39. Agarwal OP. Advanced practical organic chemistry. 26th ed. India: GOEL Publishing House; 2019.
40. Methods for identification of Herbals-HPTLC Association. Camellia sinensis. Available from: https://www.hptlc-association.org/methods/methods_for_identification_of_herbals.cfm. [Last accessed on 04 Oct 2018]
41. Cavazzuti M. Design of experiments. In: Cavazzuti M, editor. Optimization methods: from theory to design. 1st ed. Berlin: Springer; 2013. p. 13-42.
42. Sachan R, Parashar T, Singh V, Singh G, Tyagi S, Patel C. Drug carrier transfersomes: a novel tool for transdermal drug delivery system. Int J Res Dev Pharm L Sci. 2013;2:309-16.
43. Kunasekaran V, Krishnamoorthy K. Compatibility studies of rasagiline mesylate with selected excipients for an effective solid lipid nanoparticles formulation. Int J Pharm Pharm Sci. 2015;7:73-80.
44. Tsai MJ, Wu PC, Huang YB, Chang JS, Lin CL, Tsai YH. Baicalein loaded in tocol nanostructured lipid carriers (tocol NLCs) for enhanced stability and brain targeting. Int J Pharm. 2012;423(2):461-70. doi: 10.1016/j.ijpharm.2011.12.009, PMID 22193056.
45. Pardeike J, Weber S, Haber T, Wagner J, Zarfl HP, Plank H. Development of an itraconazole-loaded nanostructured lipid carrier (NLC) formulation for pulmonary application. Int J Pharm. 2011;419(1-2):329-38. doi: 10.1016/j.ijpharm.2011.07.040, PMID 21839157.
46. Nagasamy VD, Kalyani K, Tulasi K, Swetha PV, Ali SKA, Kiran HC. Transfersomes: a novel technique for transdermal drug delivery. Int J Res Pharm Nano Sci. 2014;3:266-76.
47. Walve JR, Bakliwal SR, Rane BR, Pawar SP. Transfersomes: a surrogated carrier for transdermal drug delivery system. Int J Appl Biol PharmTechnol. 2011;2:204-13.
48. Sheo DM, Shweta A, Ram CD, Ghanshyam M, Girish K, Sunil KP. Transfersomes-a novel vesicular carrier for enhanced transdermal delivery of stavudine: development, characterization and performance evaluation. J Sci Specul Res. 2010;1:30-6.
49. M VL, Zafaruddin MD, Kuchana V. Design and characterization of transferosomal gel of repaglinide. Int Res J Pharm. 2015;6(1):38-42. doi: 10.7897/2230-8407.0619.
50. Darusman F, Raisya R, Priani SE. Development, characterization, and performance evaluation of transfersome gel of ibuprofen as a transdermal drug delivery system using nanovesicular carrier. Drug Invent Today. 2018;10:3750-5.
51. Khan MA, Pandit J, Sultana Y, Sultana S, Ali A, Aqil M. Novel carbopol-based transfersomal gel of 5-fluorouracil for skin cancer treatment: *in vitro* characterization and *in vivo* study. Drug Deliv. 2015;22(6):795-802. doi: 10.3109/10717544.2014.902146, PMID 24735246.
52. Mishra N, Rana K, Seelam SD, Kumar R, Pandey V, Salimath BP. Characterization and cytotoxicity of pseudomonas mediated rhamnolipids against breast cancer MDA-MB-231 cell line.
53. OECD. Guideline 404 for Testing of Chemicals. Acute dermal irritation. Corrosion; 2015.
54. Shinde U, Pokharkar S, Modani S. Design and evaluation of microemulsion gel system of nadifloxacin. Indian J Pharm Sci. 2012;74(3):237-47. doi: 10.4103/0250-474X.106066, PMID 23439454.
55. Uttley M, Van Abbe NJ. Primary irritation of the skin: mouse ear test and human patch test procedures. J Soc Cosmet Chem. 1973;24:217-27.
56. Chanda S, Nagani K. *In vitro* and *in vivo* methods for anticancer activity evaluation and some Indian medicinal plants possessing anticancer properties: an overview. J Pharmacogn Phytochem. 2013;2:140-52.
57. Bharadwaj R, Haloi J, Medhi S. Topical delivery of methanolic root extract of Annona reticulata against skin cancer. S Afr J Bot. 2019;124:484-93. doi: 10.1016/j.sajb.2019.06.006.
58. Kowalczyk MC, Kowalczyk P, Tolstykh O, Hanausek M, Walaszek Z, Slaga TJ. Synergistic effects of combined phytochemicals and skin cancer prevention in SENCAR mice. Cancer Prev Res. 2010;3(2):170-8. doi: 10.1158/1940-6207.CAPR-09-0196.
59. Das MK, Kumar R. Development of curcumin nanoniosomes for skin cancer chemoprevention. Int J ChemTech Res. 2015;7:747-54.
60. Honary S, Zahir F. Effect of zeta potential on the properties of nano-drug delivery systems-a review (part 1). Trop J Pharm Res. 2013;12:255-64.
61. Opatha SAT, Titapiwatanakun V, Chutoprapat R. Transfersomes: A promising nanoencapsulation technique for transdermal drug delivery. Pharmaceutics. 2020;12(9):855. doi: 10.3390/pharmaceutics12090855, PMID 32916782.
62. Duangjit S, Opanasopit P, Rojanarata T, Ngawhi Frunpat T. Characterization and *in vitro* skin permeation of meloxicam-loaded liposomes versus transfersomes. J Drug Deliv. 2011;2011:418316. doi: 10.1155/2011/418316, PMID 21490750.
63. Patel R, Singh S, Singh S, Sheth NR, Gendle R. Development and characterization of curcumin loaded transfersome for transdermal delivery. J Pharm Sci Res. 2009;1:71-80.
64. Tyagi T, Garlapati PK, Yadav P, Naika M, Mallya A, Kandangath Raghavan AK. Development of nano-encapsulated green tea catechins: studies on optimization, characterization, release dynamics, and *in vitro* toxicity. J Food Biochem. 2021;45(11):e13951. doi: 10.1111/jfbc.13951, PMID 34569069.
65. Guo L, Santschi PH. Ultrafiltration and its applications to sampling and characterisation of aquatic colloids. In: Wilkinson KJ, Lead JR, editors. Environmental colloids and particles: behaviour, separation and characterisation. Chichester: John Wiley & Sons; 2006. p. 159-221.
66. Rangwala S, Tsai KY. Roles of the immune system in skin cancer. Br J Dermatol. 2011;165(5):953-65. doi: 10.1111/j.1365-2133.2011.10507.x, PMID 21729024.
67. Lippitz BE, Harris RA. Cytokine patterns in cancer patients: a review of the correlation between interleukin 6 and prognosis. Oncoimmunology. 2016;5(5):e1093722. doi: 10.1080/2162402X.2015.1093722, PMID 27467926.
68. Balkwill F. Tumour necrosis factor and cancer. Nat Rev Cancer. 2009;9(5):361-71. doi: 10.1038/nrc2628, PMID 19343034.

Front Bioeng Biotechnol. 2021;9:761266. doi: 10.3389/fbioe.2021.761266, PMID 34950641.